DEVELOPMENT AND VALIDATION OF A FINITE ELEMENT DUMMY LOWER LIMB MODEL FOR UNDER-BODY BLAST APPLICATIONS

Wade A. Baker

Thesis submitted to the faculty of Virginia Polytechnic Institute and State University in partial fulfillment of the requirements for the degree of

MASTER OF SCIENCE

In

Biomedical Engineering

Costin D. Untaroiu, Chair

Mostafiz Chowdhury

Warren N. Hardy

Andrew R. Kemper

June 28th, 2017

Blacksburg, VA

Keywords: finite element model, anthropomorphic test device, material characterization, under-body blast, improvised explosive device, impact biomechanics

Development and Validation of a Finite Element Dummy Lower Limb Model for Under-Body Blast Applications

Wade A. Baker

ABSTRACT

Anthropomorphic test devices (ATDs) are surrogates designed to predict the loads and articulations of a human. As a result of the increased incidence of improvised explosive device (IED) attacks that targeted military vehicles in recent conflicts, the US Army is interested in studying blast mitigation countermeasures. Therefore, a new ATD is being developed for use in under-body blast (UBB) experiments. A finite element (FE) model of the novel ATD was developed to inform the design of the dummy and aid researchers interested in implementing the ATD in harsh loading environments. This study focuses on the development and application of an FE model of the dummy lower limb (leg, foot, ankle).

To build strain rate-dependent FE models, the polymeric materials in the lower limb were characterized in uniaxial tension and compression at rates ranging from quasi-static to highly dynamic. Vertical impact experiments were conducted on the isolated dummy lower limb to provide data for validation of the FE model. The lower limb model was then assessed as part of a whole-body FE model of the ATD by simulating vertical loading experiments.

The material characterization experiments were simulated and the material models accurately replicated the rate-dependent behavior. The lower limb model accurately predicted the kinematic and kinetic responses measured in component and whole-body experiments. Results from validation and verification simulations suggest that the model is ready for use in future studies such as design of experiments, strength of design, or optimization.

Development and Validation of a Finite Element Dummy Lower Limb Model for Under-Body Blast Applications

Wade A. Baker

GENERAL AUDIENCE ABSTRACT

An under-body blast (UBB) refers to the use of a roadside explosive device to target a vehicle and its occupants. During Operation Iraqi Freedom, improvised explosive devices (IEDs) accounted for an estimated 63% of US fatalities. Furthermore, advancements in protective equipment, combat triage, and treatment have caused an increase in IED casualties surviving with debilitating injuries. Military vehicles have been common targets of IED attacks because of the potential to inflict multiple casualties.

Anthropomorphic test devices (ATDs) are mechanical human surrogates designed to transfer loads and display kinematics similar to a human subject. ATDs have been used successfully by the automotive industry for decades to quantify human injury during an impact and assess safety measures. Currently the Hybrid III ATD is used in live-fire military vehicle assessments. However, the Hybrid III was designed for frontal impacts and demonstrated poor biofidelity in vertical loading experiments.

To assess military vehicle safety and make informed improvements to vehicle design, a novel Anthropomorphic Test Device (ATD) was developed and optimized for vertical loading. ATDs, commonly referred to as crash dummies, are designed to estimate the risk of injuries to a human during an impact. The main objective of this study was to develop and validate a Finite Element (FE) model of the ATD lower limb.

ACKNOWLDGEMENTS

I would first like to thank my advisor, Costin Untaroiu, for his unequivocal support and for giving me the opportunity to participate in meaningful research. I would like to thank Mostafiz Chowdhury and all the members of my committee for their guidance and support. Thank you to all the collaborators on this project, namely the people at Corvid Technologies and the Johns Hopkins Applied Physics lab that provided guidance. Thank you to all the students, faculty and staff in the VT-WFU School of Biomedical Engineering and Sciences. Each of you has helped me in some way and I will always be grateful for the support I received. Lastly, I would like to thank my mom, dad, brother and sister for their lifelong support.

ATTRIBUTION

Several colleagues aided in the writing and research behind the chapters presented as part of this thesis. A brief description of their contribution is included here.

Chapter 2: MECHANICAL CHARACTERIZATION AND FINITE ELEMENT IMPLEMENTATION OF THE SOFT MATERIALS USED IN A NOVEL ANTHROPOMETRIC TEST DEVICE FOR SIMULATING UNDERBODY BLAST LOADING

Chapter 2 was accepted for publication in the *Journal of the Mechanical Behavior of Biological Materials*.

Costin D. Untaroiu, (Center for Injury Biomechanics, Department of Biomedical Engineering and Mechanics), is an associate professor of biomedical engineering and mechanics at Virginia Tech. Dr. Untaroiu was a co-author on this paper, investigator for the contracts supporting the research, and contributed editorial comments.

Dawn M. Crawford, (US Army Research Laboratory) is a research engineer of the Army Research Laboratory specializing in material science. Dr. Crawford was a co-author on this paper and was a point of contact for information regarding polymer experiments.

Mostafiz R. Chowdhury (US Army Research Laboratory) is a research engineer for the US Army Research Laboratory and member of the WIAMan Engineering Office. Dr. Chowdhury leads the Modeling and Simulation team for the WIAMan project. Dr. Chowdhury is a co-author on this paper and contributed editorial comments.

Chapter 3: A FINITE ELEMENT MODEL OF AN ANTHROPOMETRIC TEST DEVICE LOWER LIMB TO ASSESS RISK OF INJURIES DURING VERTICAL ACCELERATIVE LOADING

Chapter 3 was submitted for publication in *Medical Engineering and Physics*.

Costin D. Untaroiu, (Center for Injury Biomechanics, Department of Biomedical Engineering and Mechanics), is an associate professor of biomedical engineering and mechanics at Virginia Tech. Dr. Untaroiu was a co-author on this paper, investigator for the contracts supporting the research, and contributed editorial comments.

Mostafiz R. Chowdhury (US Army Research Laboratory) is a research engineer for the US Army Research Laboratory and member of the WIAMan Engineering Office. Dr. Chowdhury leads the Modeling and Simulation team for the WIAMan project. Dr. Chowdhury is a co-author on this paper and contributed editorial comments.

Chapter 4: VALIDATION OF A BOOTED FINITE ELEMENT MODEL OF THE WIAMAN ATD LOWER LIMB IN COMPONENT AND WHOLE-BODY VERTICAL LOADING IMPACTS WITH AN ASSESSMENT OF THE BOOT INFLUENCE MODEL ON RESPONSE

Chapter 4 was submitted for publication in *Traffic Injury Prevention.*

Costin D. Untaroiu, (Center for Injury Biomechanics, Department of Biomedical Engineering and Mechanics), is an associate professor of biomedical engineering and mechanics at Virginia Tech. Dr. Untaroiu was a co-author on this paper, investigator for the contracts supporting the research, and contributed editorial comments.

Mostafiz R. Chowdhury (US Army Research Laboratory) is a research engineer for the US Army Research Laboratory and member of the WIAMan Engineering Office. Dr. Chowdhury leads the Modeling and Simulation team for the WIAMan project. Dr. Chowdhury is a co-author on this paper and contributed editorial comments.

TABLE OF CONTENTS

LIST OF TABLES

LIST OF FIGURES

CHAPTER 1 : INTRODUCTION

1.1 Lower Limb Injuries in Underbody Blasts

An under-body blast (UBB) refers to the use of a roadside explosive device to target a vehicle and its occupants. During Operation Iraqi Freedom, improvised explosive devices (IEDs) accounted for an estimated 63% of deaths to US forces[1,2]. Furthermore, advancements in protective equipment, combat triage, and treatment have caused an increase in IED casualties surviving with debilitating injuries[3]. Military vehicles have been common targets of IED attacks because of the potential to inflict multiple casualties[4].

Injuries to the lower limb (foot-ankle-tibia complex) were often reported for a UBB event due to the proximity of the lower limb to the vehicle floor[5,6]. A review of 500 UBB casualties found approximately 200 sustained foot-ankle injuries[7], representing the most commonly injured region. Calcaneus fractures were reported in several studies as the most common post-mortem human surrogate (PMHS) injury recorded in simulated UBB impact experiments[8-10]. Talus and distal tibia fractures were also observed. Blunt axial loads imparted by rapid floor deformation was the most common mechanism of lower limb UBB injuries[4].

In current vehicle assessment tests, lower limb injury risk is determined by comparing peak compressive force recorded in the tibia of an anthropomorphic test device (ATD) to injury probability curves established from PMHS experiments[11]. Extensive research has been performed to understand lower limb injury tolerances[12-15], but the vast majority of research has been focused on automotive collision environments. An increased understanding of human musculoskeletal tolerances related to the UBB environment is needed to effectively engineer UBB safety countermeasures.

1.2 Anthropomorphic Test Devices for Military Vehicle Safety Applications

Anthropomorphic test devices (ATDs) are mechanical human surrogates designed to transfer loads and display kinematics similar to a human subject. ATDs have been used successfully by the automotive industry for decades to quantify human injury during an impact and assess safety measures. Currently the Hybrid III ATD (Humanetics, Plymouth, MI) is used in live-fire military vehicle assessments[16]. However, the Hybrid III was designed for frontal impacts and demonstrated overly-stiff behavior in vertical loading experiments[17]. The loads associated with a UBB differ from automotive impacts in direction, magnitude and duration[18]. Additionally, military vehicle occupants have a more upright posture than automotive occupants. The Military Lower Extremity (MIL-LX, Humanetics, Plymouth, MI) is a lower limb surrogate designed for use in a UBB environment[19]. The injury threshold in the MIL-LX is 2.6 kN measured at the upper tibia load cell. During its development, the MIL-LX was calibrated by changing the tibia compliant element (length & elastomer type) to match the cadaveric data at an impact speed of 7.1 m/s [19] and has shown to be overloaded at higher impact severities[20].

Currently the United States Army Research Laboratory is leading an effort to develop a novel ATD for use in live-fire tests and vehicle development efforts. The Warrior Injury Assessment Manikin (WIAMan) will be the first whole-body ATD designed for military vehicle blast testing[21]. The WIAMan lower limb (WIAMan-LL) including the foot-ankle-tibia was designed as a maturation of the existing MIL-LX (Figure 1.1d). The design features a straight tibia shaft. A 40 mm compliant element located in the tibia and three polymeric components in the foot soften the response. A full anthropometry analysis of the warrior was performed[22]. A statistical shape model from foot was developed from scans of 107 male soldiers to recommend appropriate

mid-size anthropometry for the WIAMan foot[23], an improvement over current ATD foot geometry (Figure 1).

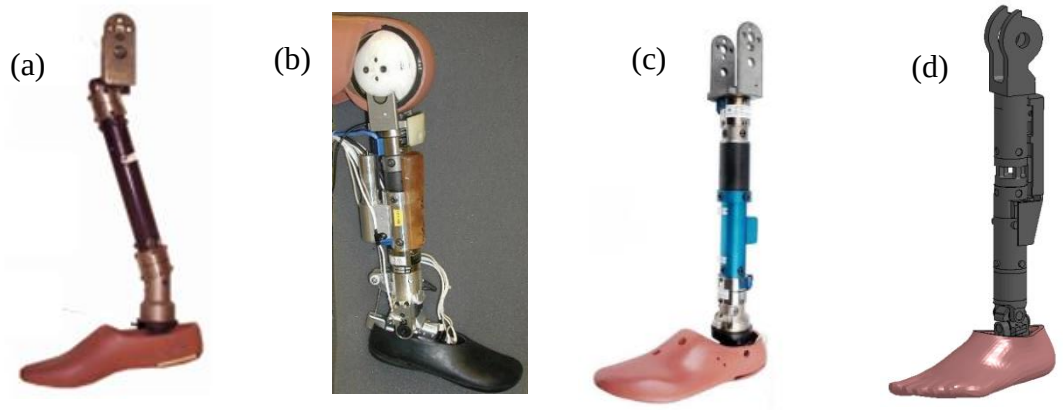

Figure 1.1 Comparison of existing ATD lower limb geometry with the WIAMan-LL. (a) Hybrid III (b) THOR-Lx/ HIIIr (c) MIL-LX (d) WIAMan-LL

1.3 Finite Element Analysis in Injury Biomechanics

ATDs and human cadavers have been used to study the response of the human body to various impacts. While both approaches offer valuable insight into the biomechanics of injury, the high costs and complications associated with testing decreases the applicability of these human surrogates. In injury biomechanics, finite element (FE) models of ATDs and humans have proven to be cost-effective substitutes for applications involving the physical surrogate[24-26]. Models can accurately simulate complex impact scenarios without the limitations associated with testing. In order to use FE models as design tools, they must first be validated against experiments conducted in the intended loading environment.

A validated numerical model offers several advantages over the physical ATD. The low cost of running simulations offer a platform for sensitivity analysis and design optimization studies that

are not feasible through physical experimentation. Also, the harsh loading environments associated with dynamic testing could cause unwanted damage to an ATD. The ability of an FE model to predict local stresses and strains make them a valuable tool for determining the strength of design of ATD components in these harsh environments. Human FE models can be used to predict the type and severity of an injury to bony or soft tissue using localized injury criteria.

The development of the WIAMan ATD includes the development, verification and validation of an FE model of the entire device. A ground up approach to verification and validation was taken[27], in which the model was validated in stages including material level, sub-system level, and system level.

1.4 Brief Summary of Chapters

The following three chapters are based on manuscripts prepared for dissemination in academic journals and reflect the work done for completion of this Master's Thesis. A brief summary of each chapter is given below.

Chapter 2: **Mechanical Characterization and Finite Element Implementation of the Soft Materials Used in a Novel Anthropomorphic Test Device for Simulating Underbody Blast Loading**

Eight soft materials in the Warrior Injury Assessment Manikin were characterized in uniaxial tension and compression to understand their viscoelastic behavior. Using the response of each material at strain rates ranging from 0.01-1000s^{-1}, rate-dependent finite element models were developed for each material. The LS-Dyna material models were validated in uniaxial tension and compression before being incorporated into a model of the ATD.

Chapter 3: **A Finite Element Model Of An Anthropometric Test Device Lower Limb To Assess Risk Of Injuries During Vertical Accelerative Loading**

A finite element model of the WIAMan lower limb was developed for LS-Dyna (LSTC, Livermore, CA). All parts of the ATD including hardware and instrumentation were explicitly modeled. Viscoelastic models of the soft components were assigned based on the work performed in Chapter 2. Experiments conducted on two under-body blast simulators were modeled to validate the ATD lower limb (unbooted) model.

Chapter 4: **Validation Of A Booted Finite Element Model Of The Wiaman Atd Lower Limb In Component And Whole-Body Vertical Loading Impacts With An Assessment Of The Boot Influence Model On Response**

The unbooted lower limb model developed and validated in Chapter 2 and Chapter 3 was fitted with a military combat boot. Experiments using the Vertically Accelerated Load Transfer System (VALTS) were simulated to validate the FE model. Then, the booted lower-limb model was incorporated into a whole-body model[28] of the ATD. The performance of the lower-limb was assessed as a component of the full ATD.

1.5 References

1. Belmont P, Schoenfeld AJ, Goodman G. Epidemiology of combat wounds in Operation Iraqi Freedom and Operation Enduring Freedom: orthopaedic burden of disease. *J Surg Orthop Adv.* 2010;19(1):2-7.
2. Bird SM, Fairweather CB. Military fatality rates (by cause) in Afghanistan and Iraq: a measure of hostilities. *International journal of epidemiology.* 2007;36:841-846.
3. Nelson TJ, Clark T, Stedje-Larsen ET, et al. Close proximity blast injury patterns from improvised explosive devices in Iraq: a report of 18 cases. *Journal of Trauma and Acute Care Surgery.* 2008;65(1):212-217.
4. Ramasamy A, Masouros SD, Newell N, et al. In-vehicle extremity injuries from improvised explosive devices: current and future foci. *Philosophical Transactions of the Royal Society B: Biological Sciences.* 2011;366(1562):160-170.

5. Ramasamy MA, Hill CAM, Masouros S, et al. Outcomes of IED foot and ankle blast injuries. *J Bone Joint Surg Am.* 2013;95(5):e25.
6. Owens BD, Kragh Jr JF, Macaitis J, Svoboda SJ, Wenke JC. Characterization of extremity wounds in operation Iraqi freedom and operation enduring freedom. *Journal of orthopaedic trauma.* 2007;21(4):254-257.
7. Pintar FA. *Biomedical analyses, tolerance, and mitigation of acute and chronic trauma.* DTIC Document;2012.
8. McKay BJ, Bir CA. Lower extremity injury criteria for evaluating military vehicle occupant injury in underbelly blast events. *Stapp car crash journal.* 2009;53:229.
9. Bailey AM, McMurry TL, Poplin GS, Salzar RS, Crandall JR. Survival model for foot and leg high rate axial impact injury data. *Traffic Inj Prev.* 2015;16(sup2):S96-S102.
10. Gallenberger K, Yoganandan N, Pintar F. Biomechanics of foot/ankle trauma with variable energy impacts. *Annals of advances in automotive medicine.* 2013;57:123.
11. Newell N, Masouros SD, Ramasamy A, et al. Use of cadavers and anthropometric test devices (ATDs) for assessing lower limb injury outcome from under-vehicle explosions. 2012.
12. Funk JR, Crandall JR, Tourret LJ, et al. The Axial Injury Tolerance of the Human Foot/Ankle Complex and the Effect of Achilles Tension. *Journal of Biomechanical Engineering.* 2002;124(6):750-757.
13. Yoganandan N, Pintar FA, Kumaresan S, Boynton MD. Axial impact biomechanics of the human foot-ankle complex. *Journal of biomechanical engineering.* 1997;119:433-437.
14. Nyquist GW, Cheng R, El-Bohy AA, King AI. *Tibia bending: strength and response.* SAE Technical Paper;1985. 0148-7191.
15. Kuppa S, Wang J, Haffner M, Eppinger R. Lower extremity injuries and associated injury criteria. Paper presented at: 17th ESV Conference, Paper2001.
16. *Procedures for Evaluating the Protection Level of Armoured Vehicles - IED Threat.* NATO;2014.
17. Bir C, Barbir A, Dosquet F, Wilhelm M, van der Horst M, Wolfe G. Validation of lower limb surrogates as injury assessment tools in floor impacts due to anti-vehicular land mines. *Military medicine.* 2008;173(12):1180-1184.
18. Scherer R, Felczak C, Halstad S. Vehicle and Crash Dummy Response to an Underbelly Blast Event. *RDECOM-TARDEC Unclassified Public Release.* 2011.
19. McKay BJ. *Development of Lower Extremity Injury Criteria and Biomechanical Surrogate to Evaluate Military Vehicle Occupant Injury During an Explosive Blast Event*. Detroit, MI, USA, Wayne State University; 2010.
20. Pandelani T, Sono T, Reinecke J, Nurick G. Impact loading response of the MiL-Lx leg fitted with combat boots. *International Journal of Impact Engineering.* 2016;92:26-31.
21. Pietsch HA, Bosch KE, Weyland DR, et al. Evaluation of WIAMan Technology Demonstrator Biofidelity relative to Sub- Injurious PMHS Response in Simulated Under-body Blast Events. *Stapp car crash journal.* 2016;60.
22. Reed MP. *Development of Anthropometric Specifications for the Warrior Injury Assessment Manikin (WIAMan).* DTIC Document;2013.
23. Reed MP, Ebert SM, Corner BD. Statistical Analysis to Develop a Three-Dimensional Surface Model of a Midsize-Male Foot. *US Army TARDEC.* 2013.

24. Putnam JB, Untaroiu CD, Littell J, Annett M. Finite Element Model of the THOR-NT Dummy under Vertical Impact Loading for Aerospace Injury Prediction: Model Evaluation and Sensitivity Analysis. *Journal of the American Helicopter Society.* 2015;60(2):1-10.
25. Untaroiu CD. *Development and Validation of a Finite Element Model of Human Lower Limb: Including Detailed Geometry, Physical Material Properties, and Component Validations for Pedestrian Injuries*, University of Virginia; 2005.
26. Untaroiu CD, Yue N, Shin J. A Finite Element Model of the Lower Limb for Simulating Automotive Impacts. *Annals of Biomedical Engineering.* 2013;41:513-526.
27. Schwer LE. Guide for verification and validation in computational solid mechanics. 2009.
28. Armiger R, Boyle M, Gayzik F, Merkle A, Chowdhury M. The Development of a Virtual WIAMan for Predicting Occupant Injury and Vehicle Performance. Paper presented at: The Ground Vehicle Survivability Symposium, ; Nov. 15-17, 2016; Fort Benning, GA.

CHAPTER 2 : MECHANICAL CHARACTERIZATION AND FINITE ELEMENT IMPLEMENTATION OF THE SOFT MATERIALS USED IN A NOVEL ANTHROPOMORPHIC TEST DEVICE FOR SIMULATING UNDERBODY BLAST LOADING

Wade A. Baker, Costin D. Untaroiu, Dawn M. Crawford, Mostafiz R. Chowdhury

Accepted for publication in the Journal of the Mechanical Behavior of Biomedical Materials

2.1 Abstract

Soft materials (e.g. polymers) are widely used in biomechanical devices to represent the nonlinear viscoelastic properties inherent in biological soft tissues. Knowledge of their mechanical properties is used to inform design choices and develop accurate finite element (FE) models of human surrogates. The goal of this study was to characterize the behavior of eight polymeric materials used in the design of a novel anthropomorphic test device (ATD) and implement these materials in an FE model of the ATD.

Tensile and compressive tests at strain rates ranging from 0.01 s^{-1} to 1000 s^{-1} were conducted on specimens from each material. Stress-strain relationships at discrete strain rates were used to define strain rate-dependent hyper-elastic material models in a commercial finite element solver. Then, the material models were implemented into an FE model of the ATD. The performance of the material models in the FE model was evaluated by simulating experiments that were conducted on the ATD lower limb.

The material characterization tests revealed viscoelastic strain rate-dependent properties in the flesh and compliant elements of the ATD. Higher modulus polymers exhibited rate-dependent, strain-hardening properties. A strong agreement was seen between the material model simulations and corresponding experiments. In component simulations, the materials performed well and the model reasonably predicted the forces observed in experiments.

2.2 Introduction

Anthropomorphic test devices (ATDs) have been used in automotive safety research since the 1970s to predict injuries[1]. ATDs must repeatedly perform under a dynamic range of loading rates and reliably distinguish between injuries ranging from minor to severe. Biofidelity is an assessment of a devices' ability to replicate the kinetics and kinematics of a human subjected to identical loads [2]. Automotive ATDs are suitable for impacts where the principle direction of force comes from the front, side or rear [3-5]. However, during the recent military conflicts in Iraq and Afghanistan, improvised explosive devices (IEDs) accounted for the most death and injury to Coalition troops [6]. Military vehicles were common targets of an IED attack because of their susceptibility to underbody-blasts and the potential to inflict multiple casualties [7,8]. Current whole-body ATDs have been shown to exhibit poor biofidelity due to overly-stiff behavior when subjected to highly accelerative vertical loads [9-11]. To address the growing threat IEDs pose to vehicle occupants, the Warrior Injury Assessment Manikin (WIAMan) project was commissioned by the US Department of Defense. The WIAMan ATD must demonstrate biofidelity with respect to a human soldier subjected to varying severities of in-vehicle underbody blast exposure.

ATD biofidelity is strongly dependent on the viscoelastic properties of its soft components representing the flesh and bony structures. Polymeric components are often included in an ATD to simulate complex properties of human soft tissues. Polymer components were used extensively in the development of an advanced automotive trauma assessment device, the Test Device for Human Occupant Restraint (THOR), to achieve desired levels of biofidelity and durability [12-16]. Updates to the six year-old Hybrid-III pelvis involved softening of the surrounding vinyl flesh material to improve the ATD's ability to assess child restraint systems [17]. The military lower extremity (MIL-LX) (Humanetics, Plymouth, MI) surrogate has a compression absorber in the

tibia shaft to improve biofidelity during vertical impacts [18,19]. The current WIAMan design also includes numerous polymeric parts to meet biofidelic requirements. The loading rates associated with under-vehicle explosions are not well established in the literature. In addition, models of polymeric materials used in current ATDs are not published mostly due to proprietary information. A range of reported values (1 m/s – 80.5 m/s) for vehicle floor deformation velocity show the uncertainty associated with blast tests of this nature [20,21]. Initial simulations of full-body WIAMan ATD experiments within its intended loading environment indicate maximum strain rates in the polymeric components are in the range of 100 – 200 s^{-1}. These rates were estimated in simulations where hyper-elastic material models were assigned to polymer components based on preliminary characterization tests. However, these findings have not been validated experimentally. It is therefore necessary to characterize the polymeric materials under a large range of strain-rates, which should include both static and high dynamic loading rates. A finite element (FE) model of the WIAMan is being developed to be used in low cost simulation of under-body impact scenarios. To predict responses of the physical dummy, the FE model must be able to replicate the viscoelastic behavior of its polymer components. A thorough understanding of the mechanical behavior of these polymers is required to develop accurate computational models of the ATD.

In this study, eight polymer materials are characterized by uniaxial compression and tension tests at strain rates from 0.01 s^{-1} to approximately 1,000 s^{-1} and implemented into an FE model of the WIAMan ATD. To the author's knowledge, none of the eight materials have been characterized within the dynamic range necessary to model blast mechanics. The validated model can be used as a valuable tool for common FE tasks such as design of experiments and failure tests, which would be extremely costly to perform on a physical dummy. Material characterization data of the

eight materials is being made available to facilitate the development and improvement of future FE models.

2.3 Methods

A schematic methodology is shown for developing and determining the suitability of FE models for the soft materials in the WIAMan ATD (Fig 2.1). The following subsections provide further details to support the methodology.

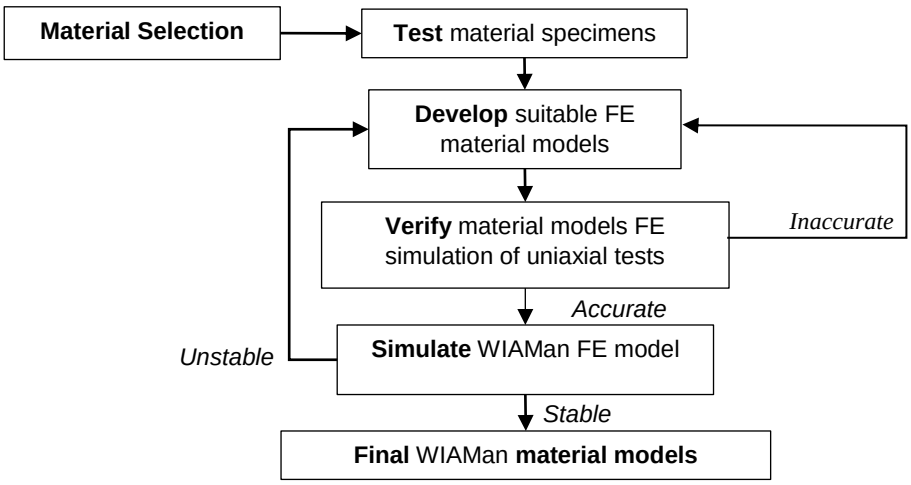

Figure 2.1 Overview of the development and evaluation of polymer material models

2.3.1 Material Overview

Eight polymeric materials used in the WIAMan ATD were chosen so the dummy response would resemble that of a human during vertical loading scenarios. There are six polyurethanes, one thermoplastic acetyl resin and one custom formulated vulcanized rubber (Table 1). The polyurethanes and acetyl resin are commercially available and were formulated according to the manufacturer's directions. A custom rubber was designed for compliant elements located in the legs and spine to accommodate flexibility and damping requirements[22]. The location of each material in the ATD along with additional material information is listed in Table 2.1. These

materials are amorphous thermosets and therefore assumed to have isotropic properties. Although some of the rubbers have carbon black filler, these are not directional and there should be nothing in the polymer morphology such as crystalline regions or fillers that align in such a way to cause directional effects.

Table 2.1 Soft material compounds, arranged by durometer, with information regarding suppliers and locations in the test device

Commercial Designation	Supplier	Material Type	Durometer	Density (g/cm^3)	Location
Proflex 30	Mouldlife (http://www.mouldlife.net/)	2-Part Polyurethane Elastomer	29 Shore A	1.04	Pelvis Flesh
F-130 A/B	BJB Enterprises (https://bjbenterprises.com)	2-Part Polyurethane Elastomer	31 Shore A	1.05	Upper Torso Flesh, Leg Flesh, Arm Flesh
XE 1031	Polymed LTD (http://www.polymedicure.com)	2-Part Polyurethane Elastomer	33 Shore A	1.06	Foot Flesh
Butyl Rubber	SACO Research /R.D Abbott Rubber	Vulcanized Elastomer (custom)	75 Shore A	1.46	Tibia Compliant Element, Spine Compliant Element
FD-70	BJB Enterprises	2-Part Semi-rigid Polyurethane	68 Shore D	1.21	Foot Plate
Rencast 6425	Huntsman (http://www.huntsman.com)	2-Part Rigid Polyurethane	67 Shore D	1.18	Coccyx
TC 892	BJB Enterprises	2-Part Rigid Polyurethane	79 Shore D	1.16	Pelvic Bone
Delrin©	Stock material	Rigid Thermoplastic (Acetyl Resin)	81 Shore D	1.41	Calcaneus Cap

2.3.2 Material Characterization Tests

Low and high strain-rate tensile and compression tests were performed on the eight materials with the intention of informing the development of FE material models. The test protocols were customized for the development of WIAMan FE material models. In all tests, the materials were not preconditioned to provide test conditions that are realistic to the condition and environment that the ATD will be used in (the ATD will not be preconditioned in service). For each material,

uniaxial tests were repeated three times per strain rate. A brief description of the test methods is provided here and can also be found in the literature [22]. A CHECK-LINE Shore A durometer (Electromatic Equipment Co, Cedarhury, NY, USA) and Rex Durometer Shore D durometer (Rex Gauge, Buffalo Grove, IL, USA) were used to characterize the hardness of the materials. Testing was performed in accordance with ASTM D-2240-05 (Type A and D) [23] on specimens with at least 12.7 mm thickness (specimens provided by suppliers). Results from durometer tests are shown in Table 1.

Low-rate uniaxial tension tests were performed at three engineering strain rates (0.01 s^{-1}, 0.1 s^{-1}, and 1.0 s^{-1}) on either an Admet 2608 (Admet, Norwood, MA, USA) electromechanical test machine or an Instron 8800 (Instron, Norwood, MA, USA) servo-hydraulic test machine depending on the required load. Specimens for 0.01 s^{-1} and 0.1 s^{-1} monotonic tests were prepared according to ASTM D638 Type IV specifications, while 1.0 s^{-1} specimens used ASTM D638 Type V geometry [24]. Specimens were stamped or waterjet cut from molded sheets. The sheets for the eight different materials were provided by the suppliers. Sheet thickness varied by material between 2.03 and 5.08 mm based on the mold used. However, thickness was consistent for each type of material (+/- 0.01 mm). The stamping and water-jet cutting procedures resulted in low standard deviations (+/- 0.5 mm^2) of specimen cross-sectional area. Crosshead controlled displacement was used to strain the specimens. Digital image correlation (DIC) using a Point Grey Gazelle camera (FLIR Integrated Imaging Solutions, Richmond, BC, Canada) was used to measure strain (10 -280 fps).

Low rate uniaxial compression tests were performed at identical strain rates as the low-rate tensile tests and used the same machines. Cylindrical specimens were used for compression testing. Low durometer (Shore A) specimens were prepared by stacking cylindrical samples cut from

material sheets to increase the aspect ratio (H:D). For all tests a lubricant, either 3 in 1 multipurpose oil or Krytox performance lubricant (GPL207) was used to reduce friction between the test specimen and instrument plates to nearly zero which minimized the adverse effect of friction on the stress-strain curve. No slipping was observed between stacked specimens. The compressive specimen dimensions for each material were: soft polyurethanes diameter (D) = 8.1 mm, stacked height (SH) = 9.5 mm); butyl rubber D = 11.2 mm, SH = 7.3 mm; rigid polyurethanes and Delrin D = 9 mm, H = 9 mm. Negligible variation of the specimen dimensions was observed for each experiment. Specimens were strained to near 50% using crosshead controlled displacement. An axial extensometer (Model 3542, Epsilon Technology, Jackson, WY, USA) was used to measure strain.

High rate tension and compression tests were performed using a drop tower (Veryst Engineering LLC, Needham Heights, MA, USA). The procedure for tension tests involved coating an ASTM Type V specimen with speckled spray paint and loading it into tension grips. A weighted sled was raised to a height, calibrated from preliminary tests, to achieve the desired strain rate. The falling sled struck the test fixture which then loaded the specimen. Three discrete strain rates between 30 s^{-1} and 400 s^{-1} were tested for each material. A high-speed camera (Photron FastCam mini UX100) was focused on the speckle pattern and the engineering strain was calculated based on DIC (30,000 fps). Compression tests were carried out by placing a cylindrical specimen between two platens. Tests were performed at two strain rates that varied per material (approximately 50 s^{-1} and 150 s^{-1}). A drop-mass procedure similar to the tension tests was used to induce downward motion of the top platen, causing the specimen to compress. Force was measured using a load cell under the bottom platen. Strain was derived from the movement of fiducial markers on the platens using a Photron UX100 high speed camera (Photron, Tokyo, Japan). Shore

A material specimens were prepared by stacking cylindrical samples, identical to the low rate compression tests. Shore D material test specimens were cylinders 6mm in diameter and height.

Split Hopkinson pressure bar (SHPB) compression tests [25] were performed to achieve very high compression strain rates (500 s^{-1} – 1000 s^{-1}). In this method, cylindrical test specimens (D = 6 mm, H = 6 mm) for the rigid Shore D durometer materials were placed between two bars called the incident and transmitted bars. A larger ratio H:D (1.5) was used for the soft Shore A rubbers. No buckling models were observed in all tests. Dynamic loading was induced by firing a striker into the 90-inch-long aluminum incident bar. A stress wave then travels the length of the incident bar where a portion of energy is transmitted to the sample and the rest is reflected. The transmitted wave travels through the specimen, inducing deformation, and into the transmitted bar. The reflected wave travels back up the incident bar. Strain gauges were used to measure strain in the bars (sampling rate from 1-5 mil. samples per sec). Elastic wave analysis was used to calculate stress and strain in the specimen from the amplitudes of the incident, transmitted and reflected waves according to established SHPB equations [26].

2.3.3 Finite Element Material Development and Validation

Several material models for rubber/foam implemented in LS-Dyna software were selected and material identification using optimization algorithms (e.g. genetic, simulated annealing, simplex, etc. [27]), were applied to fit test data. A simplified material model for rubber [28,29] showed the highest performance for all strain rates. This material model (MAT_181, LS-Dyna), implemented in the LS-DYNA solver (LSTC, Livermore, CA, USA), is based on the Ogden formulation [30]. Stress-strain curves derived from uniaxial static and dynamic tests are tabulated at discrete strain rates and the material parameters are directly identified in the model. This approach removes the need for viscous damping parameter identification.

Each FE material model of the eight polymeric materials, was qualitatively validated against test data before to be implemented in the ATD FE model. The curves assigned to the material model were derived by taking the mean of three experiments performed at certain strain rates. A single 1 mm^3 solid brick element was assigned the simplified rubber material and simulated under tension and compression at rates according to the tests. The strain rate was controlled by prescribing constant velocity to the top four nodes of the element. The bottom four nodes were constrained in the vertical direction and allow to freely expand in the lateral directions. Uniaxial force was recorded at a cross section defined at the element's center. For the unique case where original length of the specimen is 1 mm, engineering strain is calculated from the velocity-time history of deformation as follows:

$$\varepsilon = v(t)t \tag{1}$$

where ε is engineering strain, v is velocity and t is time. The cross-sectional area of the element was 1 mm^2 which means the recorded force is numerically equivalent to the engineering stress after accounting for unit conversion. Validation of the material models was done by comparing the engineering stress-strain histories of simulations to experimental data corresponding to the same strain rate. The models were considered validated if the shape, magnitude and phase of the experimental responses were reasonably predicted by the numerical models.

2.3.4 WIAMan ATD Tested Under Vertical Loading

The material models were implemented in an ATD FE model and validated against vertical test data recorded on component tests of the ATD lower leg. The Vertically Accelerated Load Transfer System (VALTS) is a test device designed to impart loads associated with under-body blasts to whole-body subjects (PMHS or ATD)[21]. A modified VALTS rig (Fig. 2.2) was used for component testing on an isolated WIAMan lower extremity (WIAMan-LX). The ATD foot was

positioned on top of a foot platen. A ballistic mass was driven into the 3.1 kg foot platen to initiate the impact. Pulse shaping was done to control the magnitude and shape of the input.

Peak floor velocities between <1 m/s and 27 m/s were identified from a series of blast events recorded in theatre [21]. It was shown that in the majority of events the peak velocities were under 10 m/s and occurred within 5 ms. Based on these results, three conditions were tested in which the WIAMan-LX was impacted at peak velocities of 2.4 m/s, 3.9 m/s, and 5.8 m/s respectively. Two tests were performed at each speed.

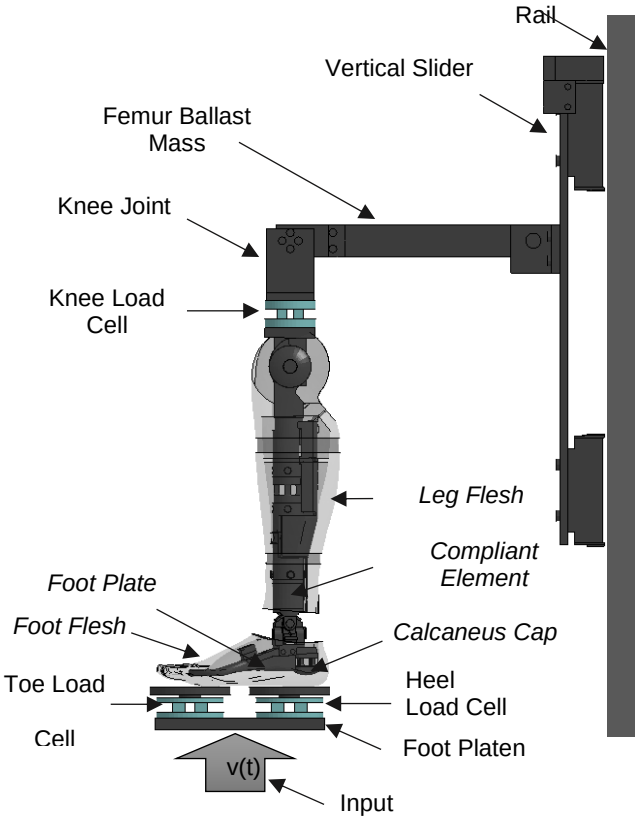

Figure 2.2 Diagram of modified VALTS rig for isolated lower extremity tests. The WIAMan-LX is pictured and the five polymer components are labeled.

2.3.5 WIAMan FE model in Simulated Vertical Loading

A preliminary FE model of the WIAMan-LX was developed previously based on geometry of the physical ATD[31]. The WIAMan-LX contains five of the eight polymer materials (foot flesh, leg flesh, compliant element, footplate, calcaneus cap) characterized in this study. The polymeric components were assigned material models validated using single element simulations. Material properties of other parts such as steel and aluminum were assigned based on available literature. The WIAMan-LX FE model was constrained to a model of the VALTS test device. The velocity of the foot platen was prescribed based on measurements from an accelerometer mounted to the center of gravity of the platen. Load cell responses at the heel, toe and knee were used to validate the WIAMan-LX FE model.

2.4 Results

Data derived from the material characterization tests showed varying degrees of rate dependent behavior in each of the eight polymers. Experimental and simulation results are shown together (Fig. 2.3) to show a validation of the simplified rubber material models.

The FE material models developed in LS-Dyna were able to reasonably predict the stress-strain relationship of the eight materials at compression strain rates between 0.01 s^{-1} and 1,000 s^{-1}. Tensile validation was performed for materials when a clear pattern of rate dependency could be seen between loading rates. For example, the flesh materials (foot, pelvis, other) exhibited negligible rate dependence in tension compared to their compressive behavior (Fig 2.3 a,e,f). For these materials, a single tensile curve was assigned based on a simple average of all tension tests. The pelvic bone was validated in tension at one quasi-static rate and one high rate. All other materials were validated at select strain rates between the lowest and highest.

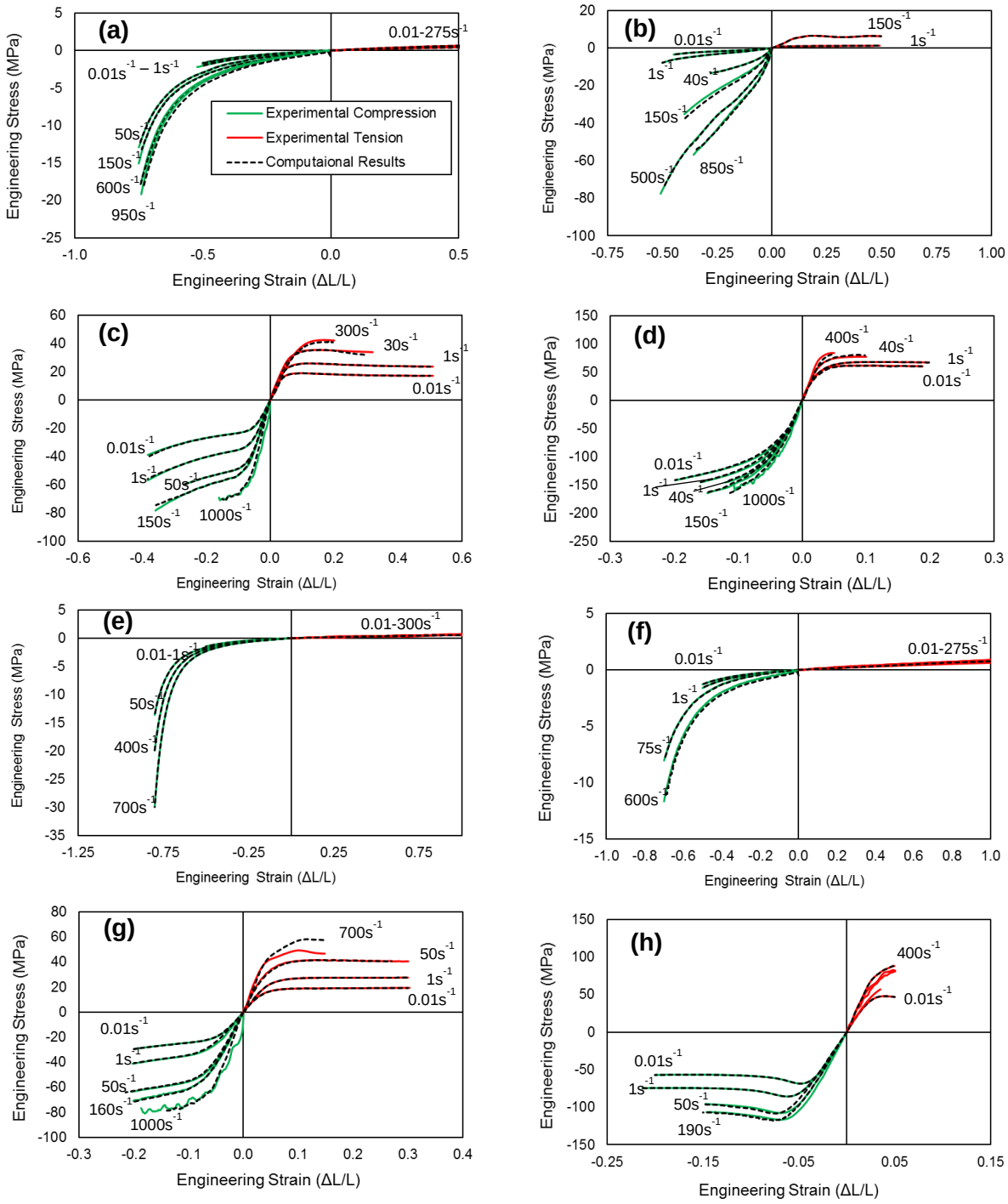

Figure 2.3Comparison of experimental data and simulation results for materials 1-8. (a) Foot flesh (b) Compliant Element (c) Footplate (d) Calcaneus Cap (e) Pelvis Flesh (f) Other Flesh (g) Tailbone (h) Pelvic Bone

The WIAMan-LX FE model was able reasonably predict the response of the experiments in terms of the force time histories at the heel, toe, and knee (Figure 2.4).

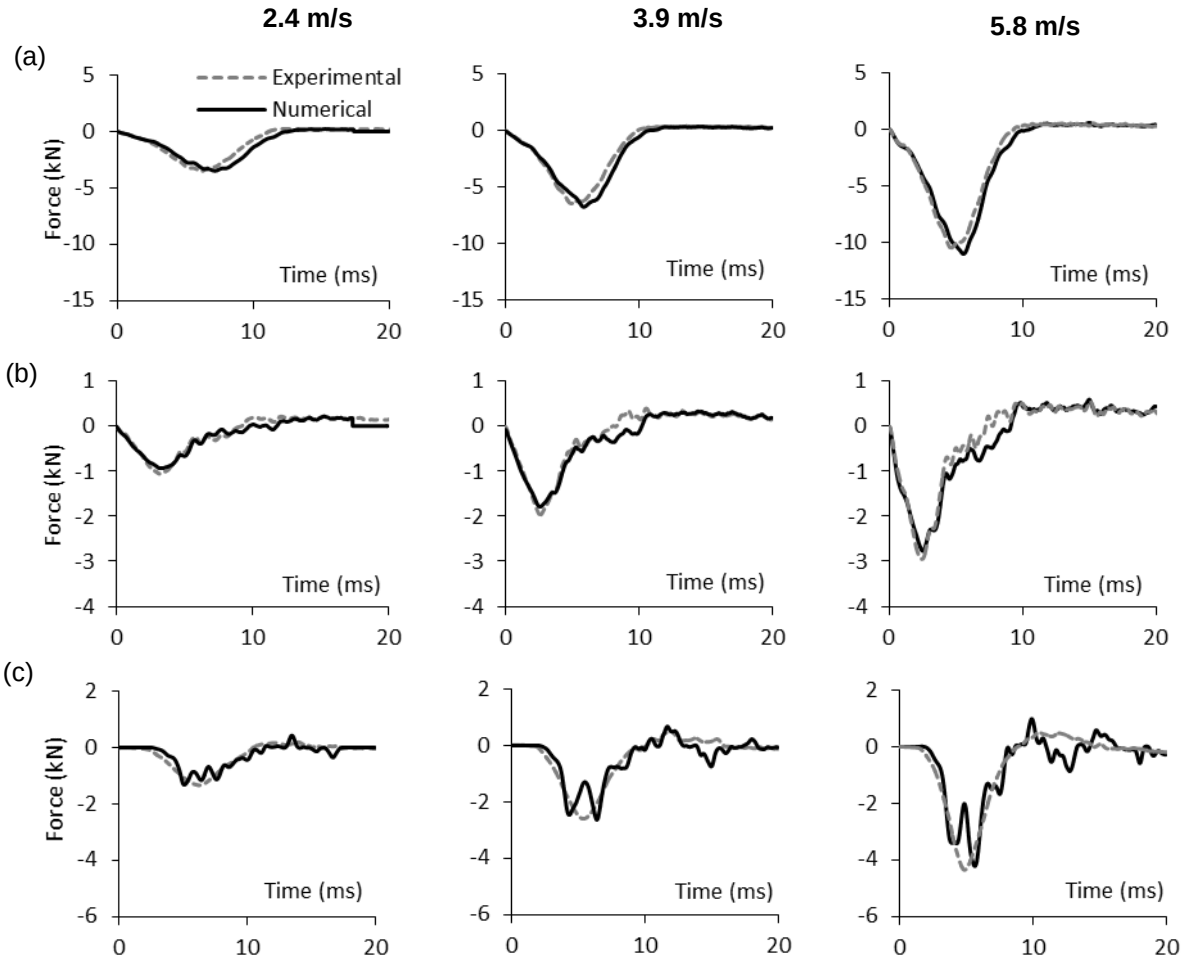

Figure 2.4 Comparison of simulations to VALTS experiments at the (a) heel (b) toe and (c) knee load cells showing accurate transfer of force through the ATD at various loading rates

2.5 Discussion

In this study, eight polymer materials were characterized to understand their nonlinear rate-dependent behavior. The materials are included in a novel ATD that is designed to predict human musculoskeletal injuries during an underbody blast. Three of the materials (foot flesh, calcaneus cap and footplate) make up components in the foot-ankle complex of the dummy, a frequently

injured body region during vertical loading scenarios[32]. The polymer materials were incorporated into components along the primary loading pathways so the ATD would exhibit human-like responses.

Strain rate dependency was observed in all eight dummy materials tested in this study. Generally, the compression data showed a rate dependent behavior which is frequently observed in the mechanical response of biological materials (e.g. lower limb flesh, [33]). Soft (Shore A) polyurethanes stiffened as they reached strains exceeding 50%. Occasionally for soft materials, the measured stress-strain curves showed an indiscernible strain rate dependence in between successive rate (e.g. from 75 s^{-1} – 150 s^{-1}). However, analyzing a larger range of strain rates (e.g. from 75 s^{-1} – 600 s^{-1}, Fig 2.3f) showed a stiffening trend. Shore D materials exhibited rate-dependent strain hardening behavior under quasi-static and dynamic loading. Although using different test methods and specimen dimensions could be considered a limitation of this study, different test methods were required to achieve the broad range of strain rates necessary for model development. The results consistently show clear trends in the data with respect to strain rate, minimizing any concern of effects from changing methods.

All specimens of the polymer components were strained at least up to 50% and the soft flesh material were strained further. The maximum strain predicted in WIAMan FE simulations was 43% in the foot flesh for the 6 m/s loading condition. Maximum strain in the compliant element was 31%. In the WIAMan compliant element, compression is limited by a bolt running through the hollow center of the element.

For each of the eight materials a simplified rubber material was developed in LS-DYNA. One benefit of using the simplified rubber material model is the ability to numerically replicate non-linear rate-dependent behavior of polymeric materials. The process of identifying hyperelastic

and viscoelastic parameters for widely used models (Ogden, Johnson-Cook, etc.) is often non-trivial and time consuming. Rather than a strain energy density function, the simplified rubber model uses a family of stress-strain curves defined at discrete strain rates to determine stress in the elements. The stress strain curves presented in this study were chosen based on their suitability for developing rate-dependent FE models. In cases where test results did show some overlap between the curves at different strain rates, the stress-strain data was not incorporated into the FE material model. For example, pelvic bone test data (Fig. 2.3h) in tension sometimes slightly overlapped at intermediary strain rates. In this case, one quasi-static curve (0.01 s^{-1}) and one high rate curve (400 s^{-1}) were tabulated in the material model. This prevents the need to manipulate the test data to suit the FE model. The model interprets between the two curves when the material deforms at intermediary strain-rates.

The WIAMan-LL contains five of the materials characterized in this study, which is more than any other sub-assembly of the WIAMan. Therefore, WIAMan-LL component experiments were simulated to assess the performance of the models developed for each of the five lower-limb polymer components. Comparing the shape, magnitude and phase of axial loads predicted by the model to experimental results, the WIAMan-LL model was able to accurately transfer axial loads. A double-peak was predicted by the model at the knee load cell for 4 m/s and 6 m/s impacts. This is believed to be from noisy contacts near the knee joint as a double-peak was not visible in either of the other two load cells during testing.

Preliminary simulation results indicated that strain rates in the WIAMan ATD would not exceed 150 s^{-1} within the intended loading environment[34]. However, these were just estimates that had not been validated experimentally. Therefore, tensile and compression tests performed on specimens from 0.01 s^{-1} to 1000 s^{-1} will produce robust FE material models that encompass the

full range of loading rates that could affect the ATD. In the 5.8 m/s VALTS simulation presented in this study, the maximum compression strain rate was 200 s^{-1} in the foot flesh. It is important to note these experiments and simulations were performed for model validation purposes without the inclusion of a combat boot. While the impact velocities are based on loading conditions observed in theatre [21], a combat boot will be used for all safety assessments involving the WIAMan which could decrease the peak levels of ATD strain and strain rate.

While the performance of other LS-Dyna material models were tested such as the Ogden and Johnson Cook[34], the simplified rubber material model (MAT_181) showed the highest capability to replicate both the tension and compression behavior of investigated polymeric materials over a large range of strain rates. Some limitations of the developed material models are the lack of a damage formulation and temperature sensitivity. In the future, damage should be added to the models based on failure and cyclic loading tests. Once live-fire testing of the ATD begins, temperature effects should be considered if numerical results fail to match experiments. The good response of material models shown in both uniaxial and lower limb component simulations suggests applying them in whole-body ATD FE models for improving the protection of vehicle occupants during under-body blast events.

2.6 Conclusions

This study focused on the development of finite element (FE) material models of eight soft materials used in a novel test device for underbody blast injury assessment. Components fabricated from these polymers align with the critical load paths when the ATD is in a normal seated posture and exposed to UBB loads. Understanding the mechanical behavior of these components is necessary to ensure the predictive capability of WIAMan FE models. A comprehensive set of uniaxial experiments was performed to characterize the materials under quasi-static and dynamic

loading rates. The constitutive laws used for modeling were chosen to capture the non-linear strain rate responses of each material. Material models underwent thorough validation by simulating tests conducted at strain rates varying from 0.01 s^{-1} to 1000 s^{-1}. The validated materials were incorporated into a FE model of the WIAMan ATD. Component tests on the isolated WIAMan lower-extremity were simulated to show the FE model's ability to predict the forces in the components of physical dummy.

2.7 Acknowledgments

Funding for the project was provided by the Army Research Laboratory. The authors would like to acknowledge Veryst Engineering LLC for performing all material tests presented in this study. The authors would also like to acknowledge the contributions of the WIAMan ATD Product Team (PT), Test and Evaluation (T&E), and WIAMan Modeling and Simulation (M&S) PT. These groups have provided test data, model feedback, and human response insight that have been instrumental in the development of a validated WIAMan model.

2.8 References

1. Crandall JR, Bose D, Forman J, et al. Human Surrogates for Injury Biomechanics Research. *Clin Anat.* 2011;24(3):362-371.
2. Mertz HJ, Irwin AL. Anthropomorphic Test Devices and Injury Risk Assessments. In: *Accidental Injury.* Springer; 2015:83-112.
3. Eppinger RH, Marcus JH, Morgan RM. *Development of dummy and injury index for NHTSA's thoracic side impact protection research program.* SAE Technical Paper;1984. 0148-7191.
4. Foster JK, Kortge JO, Wolanin MJ. *Hybrid III-a biomechanically-based crash test dummy.* SAE Technical Paper;1977. 0148-7191.
5. Davidsson J, Svensson MY, Flogård A, et al. BioRID I: a new biofidelic rear impact dummy. Paper presented at: Proceedings of the International Research Council on the Biomechanics of Injury conference1998.
6. Ramasamy A, Harrisson SE, Clasper JC, Stewart MP. Injuries from roadside improvised explosive devices. *Journal of Trauma and Acute Care Surgery.* 2008;65(4):910-914.
7. Ramasamy A, Masouros SD, Newell N, et al. In-vehicle extremity injuries from improvised explosive devices: current and future foci. *Philosophical Transactions of the Royal Society B: Biological Sciences.* 2011;366(1562):160-170.

8. Wilson C. Improvised explosive devices (IEDs) in Iraq and Afghanistan: effects and countermeasures. 2006.
9. Bir C, Barbir A, Dosquet F, Wilhelm M, van der Horst M, Wolfe G. Validation of lower limb surrogates as injury assessment tools in floor impacts due to anti-vehicular land mines. *Military medicine.* 2008;173(12):1180-1184.
10. Newell N, Masouros SD, Ramasamy A, et al. Use of cadavers and anthropometric test devices (ATDs) for assessing lower limb injury outcome from under-vehicle explosions. 2012.
11. Bailey AM, Christopher JJ, Salzar RS, Brozoski F. Comparison of Hybrid-III and Postmortem Human Surrogate Response to Simulated Underbody Blast Loading. *Journal of Biomechanical Engineering.* 2015;137(5):051009.
12. Haffner M, Eppinger R, Rangarajan N, Shams T, Artis M, Beach D. Foundations and elements of the NHTSA THOR alpha ATD design. Paper presented at: 17th ESV Conference, Paper2001.
13. Vezin P, Bruyere-Garnier K, Bermond F, Verriest J-P. Comparison of Hybrid III, Thor-alpha and PMHS Response in Frontal Sled Tests. *Stapp car crash journal.* 2002;46:1-26.
14. Ridella S, Parent D. Modifications to improve the durability, usability, and biofidelity of the THOR-NT dummy. Paper presented at: 22nd ESV Conference, Paper2011.
15. Putnam JB, Somers JT, Wells JA, Perry CE, Untaroiu CD. Development and evaluation of a finite element model of the THOR for occupant protection of spaceflight crewmembers. *Accident Anal Prev.* 2015;82:244-256.
16. Putnam JB, Somers JT, Untaroiu CD. Development, Calibration, and Validation of a Head-Neck Complex of THOR Mod Kit Finite Element Model. *Traffic Inj Prev.* 2014;15(8):844-854.
17. Klinich KD, Reed MP, Manary MA, Orton NR. Development and testing of a more realistic pelvis for the Hybrid III 6-year-old ATD. *Traffic Inj Prev.* 2010;11(6):606-612.
18. Newell N, Salzar R, Bull AM, Masouros SD. A validated numerical model of a lower limb surrogate to investigate injuries caused by under-vehicle explosions. *J Biomech.* 2016;49(5):710-717.
19. McKay BJ. *Development of Lower Extremity Injury Criteria and Biomechanical Surrogate to Evaluate Military Vehicle Occupant Injury During an Explosive Blast Event*. Detroit, MI, USA, Wayne State University; 2010.
20. Newell N, Neal W, Pandelani T, Reinecke D, Proud WG, Masouros SD. The Dynamic Behaviour of the Floor of a Surrogate Vehicle Under Explosive Blast Loading. *Journal of Materials Science Research.* 2016;5(2):65.
21. Merkle A, Voo L, Ott K, Dooley C, Carneal C. APL Status Update. Paper presented at: Medical Research Meeting Sept 11-122012; Ft. Rucker.
22. Crawford DM, Chowhurdy MR, Pietsch HA. *Mechanical Properties of Polymers Used for Anatomical Components in the Warrior Injury Assessment Manikin (WIAMan) Technology Demonstrator.* US Army Research Laboratory;2016. ARL-TR-7728.
23. ASTM. Standard Test Method for Rubber Property Durometer Hardness. In: ASTM International; 2015.
24. ASTM. Standard Test Method for Tensile Properties of Plastics. In: ASTM International; 2014.
25. Kolsky H. An investigation of the mechanical properties of materials at very high rates of loading. *Proceedings of the Physical Society Section B.* 1949;62(11):676.

26. Gray GT. Classic Split-Hopkinson Pressure Bar Testing. *Materials Park, OH: ASM International, 2000.* 2000:462-476.
27. Untaroiu CD, Meissner MU, Crandall JR, Takahashi Y, Okamoto M, Ito O. Crash reconstruction of pedestrian accidents using optimization techniques. *Int J Impact Eng.* 2009;36(2):210-219.
28. Kolling S, Bois PD, Benson D, Feng W. A tabulated formulation of hyperelasticity with rate effects and damage. *Computational Mechanics.* 2007;40(5):885.
29. Hallquist JO. LS-DYNA keyword user's manual. *Livermore Software Technology Corporation.* 2007;970.
30. Ogden R. Large deformation isotropic elasticity-on the correlation of theory and experiment for incompressible rubberlike solids. Paper presented at: Proceedings of the Royal Society of London A: Mathematical, Physical and Engineering Sciences1972.
31. Baker W, Untaroiu C, Chowdhury M. Development of a Finite Element Model of the WIAMan Lower Extremity to Investigate Under-body Blast Loads. 14th International LS-DYNA Conference; 2016; Detroit, MI.
32. Ramasamy MA, Hill CAM, Masouros S, et al. Outcomes of IED foot and ankle blast injuries. *J Bone Joint Surg Am.* 2013;95(5):e25.
33. Untaroiu CD. *Development and Validation of a Finite Element Model of Human Lower Limb: Including Detailed Geometry, Physical Material Properties, and Component Validations for Pedestrian Injuries*, University of Virginia; 2005.
34. Chowhurdy MR, Crawford DM, Shanaman M, et al. *Polymeric Material Models in the Warrior Injury Assessment Manikin (WIAMan) Anthropomorphic Test Device (ATD) Tech Demonstrator.* US Army Research Laboratory;January, 2017. ARL-TR-7927.

CHAPTER 3 : A FINITE ELEMENT MODEL OF AN ANTHROPOMETRIC TEST DEVICE LOWER LIMB TO ASSESS RISK OF INJURIES DURING VERTICAL ACCELERATIVE LOADING

Wade A. Baker[1], Costin D. Untaroiu[1], Mostafiz Chowdhury[2]

[1]Department of Biomedical Engineering and Mechanics, Virginia Tech, [2]United States Army Research Laboratory

3.1 Abstract

Improvised explosive devices (IEDs) were extensively used to target occupants of military vehicles during the conflicts in Iraq and Afghanistan. Casualties of an IED attack are highly susceptible to lower limb injuries. To assess vehicle safety and make informed improvements to vehicle design, a novel Anthropomorphic Test Device (ATD) was developed and optimized for vertical loading. ATDs, commonly referred to as crash dummies, are designed to estimate the risk of injuries to a human during an impact. The main objective of this study was to develop and validate a Finite Element (FE) model of the ATD lower limb. Appropriate materials and contacts were applied to realistically model the physical dummy. Validation is presented based on experiments performed on two different test devices designed to simulate the vertical loading experienced during an under-vehicle explosion. Correlation scores between the simulations and experiments were calculated using objective rating systems used in the field of ATD validation. Hybrid-III and post mortem human surrogate (PMHS) tests were also performed to assess the biofidelity of the ATD. The numerical lower limb is currently incorporated into a whole body model that will be used to improve the vehicle design for underbody blast protection.

3.2 Introduction

The utilization of anti-vehicular landmines and improvised explosive devices (IEDs) to target military vehicles increased significantly during the operations in Iraq and Afghanistan and presented a clear threat to US and coalition forces [1-3]. The occupant's lower limb is particularly susceptible to injury due to its proximity to the blast origin[4]. A review of 500 underbody blast casualties found 40% sustained injuries to the foot, ankle or tibia[5]. Injury to the lower limb is typically caused by rapid deformation of the vehicle floor, resulting in fracture and open wounds[6].

Military vehicles are subjected to live-fire IED tests with pass/fail criteria[7]. The ability of the vehicle to protect an occupant is determined using human surrogate ATDs. The North Atlantic Treaty Organization (NATO) currently recommends that under-belly blast (UBB) occupant survivability tests be conducted with the 50th percentile male Hybrid-III ATD outfitted with the either the Military Lower Extremity (MIL-LX) or the Denton leg (instrumented H-III lower-limb)[7,8]. However, the Hybrid-III (Humanetics, Plymouth, MI) was developed for automotive crashworthiness tests [9]. It has been shown in several studies that the Hybrid-III dummy is overly-stiff compared to cadaver responses and unsuitable for UBB loading[10-12], possibly due to the shorter duration and higher magnitude loads associated with a UBB[13-15]. Automotive crash events normally result in floor accelerations no greater than 250 *g* with loading durations of 10-50ms [16,17]. Loading from UBBs may exceed 1000 g with peak loads occurring within 5ms [18]. The Military Lower Extremity (MIL-LX) (Humanetics, Plymouth, MI) is an ATD developed to evaluate anti-vehicular landmine countermeasures. A major limitation of the MIL-LX is that it was calibrated to match PMHS data at a single impact speed of 7.1 m/s [19]. Pandelani et al. tested the MIL-LX outfitted with a combat boot at impact speeds from 2.7-10.2 m/s and found the compliant element bottomed out at higher severity loads [20].

A novel ATD is being developed by the US Army, called the Warrior Injury Assessment Manikin (WIAMan), for use in vertical loading scenarios[21]. A finite element (FE) model of the ATD is concurrently being developed. Computational FE models of ATDs have been widely used to effectively predict the responses of the ATD. The low cost, diminishing run times, and high efficacy of FE simulations are also desirable for applications, such as design of experiments, strength of design and sensitivity studies.

This study aims to develop and validate a computational model of the dummy lower limb to predict the outcome of otherwise costly experiments. The viscoelastic materials in the dummy that influence biofidelity were characterized in uniaxial tension and compression to build rate-dependent material models for finite element simulations. Component experiments were conducted on two devices designed to impart vertical under-body loading conditions. The developed model was simulated under a range of loading conditions and compared to corresponding physical experiments. Model validation was performed using two objective rating metrics from the field of ATD validation. The biofidelity of the ATD was assessed by comparison to human lower limb tests as well.

3.3 Methods

A methodology is shown for developing and evaluating the performance of the WIAMan-LX model (Fig 3.1). The following subsections provide further details to support the methodology.

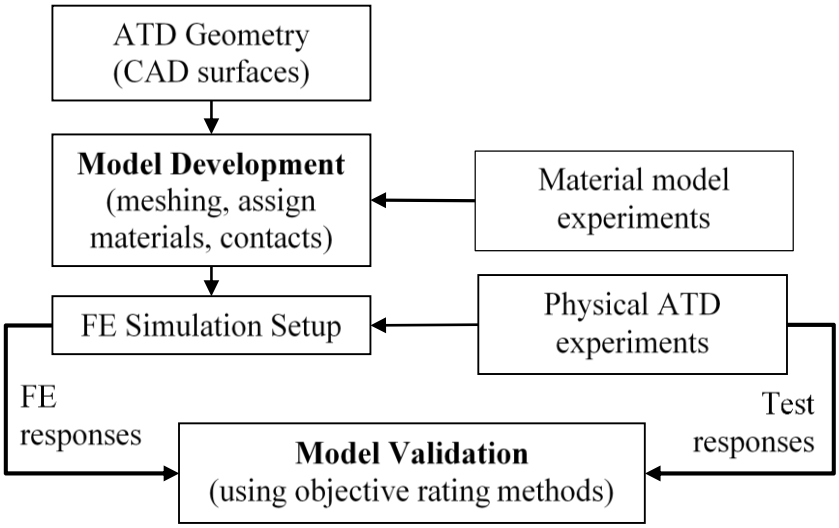

Figure 3.1 Overview of the development and evaluation of the WIAMan lower-limb finite element model

3.3.1 Development of WIAMan Lower Limb Finite Element Model

The design of WIAMan-LX (Fig. 3.2a) has a straight tibia shaft from the knee clevis to the ankle. The shaft has a built-in 40 mm long compliant element aligned to compress along the vertical loading direction. A statistical foot model[22] obtained from scans of 107 male soldiers was used as a basis for the external geometry of the foot. The ankle contains two revolute joints that separately permit motion in the sagittal (dorsiflexion/plantarflexion) and frontal (inversion/eversion) planes (Fig. 3.2b). A rotational ring built into the mid-tibia facilitates motion of the lower tibia-ankle-foot in the transverse (abduction/adduction) plane. Multiple sensors are included in the WIAMan-LX to measure the kinematics and loads at areas commonly associated with injury criteria. Six axis load cells (MG Sensors, Rheinmunster, Germany) in the tibia and calcaneus record force and moment responses of the ATD. Six degree-of-freedom (DOF) sensors (Diversified Technology Systems, Inc., Seal Beach, CA) on the foot and tibia shaft recorded linear

acceleration and rotational velocity (Fig. 3.2a). Each six DOF sensor bundled three accelerometers and three angular rate sensors.

A finite element model of the WIAMan-LX was developed (Fig. 3.2b) in LS-DYNA software (LSTC, Livermore, CA) based on CAD drawings of the physical dummy. All parts, hardware and instrumentation for the dummy were explicitly modelled to fully encompass the kinetics and kinematics involved in the impact. The rotational joints were modelled using surface contacts with a smoothing option added. Bolted connections were modelled using tied contacts. Load cells were represented using a defined cross section with responses output in a locally defined coordinate system. Six DOF accelerometers and angular rate sensors were output at a single node defined at the center of mass of each sensor array using the *CONSTRAINED_INTERPOLATION card.

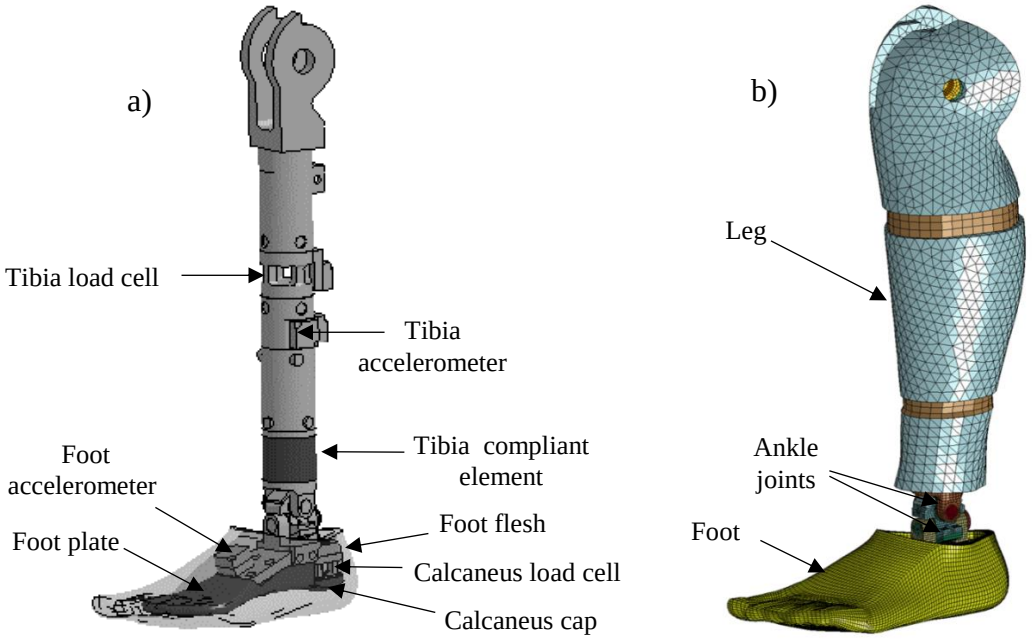

Figure 3.2 a) The main WIAMan-LX soft components of the lower limb and the instrumentation used to assess risk of injury b) WIAMan-LX FE model

Five polymeric components of the ATD (leg flesh, foot flesh, calcaneus cap, foot plate, and tibia compliant element) were selected so ATD responses match PMHS response corridors at various loading conditions[23]. A summary of the polymeric components and corresponding materials was provided (Table 1). Preliminary FE simulations of the WIAMan-ATD under vertical loading revealed the maximum strain rate in any part does not exceed 150/s. Therefore, samples of these polymeric materials were tested at strain rates 0.01-150/s. Low rate tension tests at 0.01 and 0.1 strain rate were performed on ASTM D638 Type IV specimens and tests at 1/s were done on ASTM D638 Type V specimens. Samples were strained by a crosshead controlled test apparatus (Instron 8800, Norwood, MA, USA). Digital image correlation using a Point Grey Gazelle camera (FLIR Integrated Imaging Solutions, Richmond, BC, Canada) was used to measure strain. Low rate compression tests were performed at identical strain rates as the low-rate tensile tests. An Epsilon technology (Epsilon Technology, Jackson, WY, USA) axial extensometer (Model 3542) was used to measure strain. The specimen dimensions varied slightly for each material but were generally the following geometries: soft polyurethanes diameter (D) = 8.1 mm, stacked height (SH) = 9.5mm); butyl rubber D = 11.2 mm, SH = 7.3 mm; rigid polyurethanes and Delrin D = 9 mm, H = 9 mm. Specimens were strained to 50% using crosshead controlled displacement. High rate tests in the range of 50 -150 s^{-1} were performed using a drop tower. Tension tests used ASTM Type V specimens. Compression tests used cylindrical samples with geometry equal to the low rate experiments. Strain was measured using fiducial markers located on the tower's platens by a high speed camera (FastCam mini UX100, Photron, Tokyo, Japan).

Table 3.1 Compliant parts of the WIAMan lower leg model

No.	Part Name	Material Type	Density(g/cm^3)	LS-DYNA Model
1	Foot Flesh	Polyurethane Elastomer	1.06	MAT 181
2	Leg Flesh	Polyurethane Elastomer	1.05	MAT 181
3	Calcaneus Cap	Acetal Resin	1.41	MAT 181
4	Footplate	Polyurethane Elastomer	1.21	MAT 181
5	Tibia Compressive Element	Butyl Rubber	1.46	MAT 181

A simplified rubber material [24] (MAT 181, LS-DYNA) was developed for each of the five compliant parts of the ATD. To develop the simplified rubber material, stress-strain curves from the uniaxial tension and compression tests were tabulated at discrete strain rates. To verify the simplified rubber material for each of the five components, a single element (1 mm^3) in LS-DYNA was assigned one of the five materials. Simulations were then performed where the element was deformed at constant velocities corresponding to experimental strain rates.

3.3.2 Validation of WIAMan Lower Limb Finite Element Model

The lower limb model was validated based on the test data recorded in a series of impact experiments conducted on two test rigs, which vertically loaded the physical WIAMan-LX to simulate an UBB. Experiments conducted on the Vertical Accelerator[25] (VertAc, Medical College of Wisconsin) provided one loading condition (2 m/s pre-impact velocity). Experiments using the Vertically Accelerated Load Transfer System[26,27] (VALTS, Johns Hopkins Applied Physics Lab) at three load severities (2, 4, 6 m/s pre-impact velocities) provided a second set of model validation responses. These impact severities were chosen to provide a range of severities available for validation, while preventing physical damage to the ATD.

For VertAc experiments[25] (Fig. 3.3), the specimen was positioned such that the Z axis of the tibia was set vertically and the bottom of the foot was set horizontally. A ballast mass on the rig, representing the femur, was set horizontally. Joints at the proximal and distal end of the femur bar allowed rotation about the anatomical Y-axis to approximate the knee and hip joints. In addition to WIAMan-LX experiments, the Hybrid-III lower limb and PMHS lower limbs were tested on the VertAc loading device. Six non-injurious PMHS lower limb and two Hybrid-III tests were performed. WIAMan and Hybrid-III responses were compared to PMHS responses to evaluate dummy biofidelity. Adaptors were built for the WIAMan and Hybrid-III ATDs. PMHS legs were potted in PMMA with everything below the knee intact before being attached to the test rig. A 5.4 kg impactor plate rested on a roller bearing connected to a lever arm. The impactor was in contact with the inferior surface of the foot and the center of gravity of the plate was aligned with the vertical axis of the tibia. The plate is set in motion when the opposite end of the lever arm is struck by a 61.2 kg drop mass. The maximum pre-impact velocity of the impactor plate (2 m/s) was reached 5 ms after motion was initiated. Six-axis load cells in the tibia and calcaneus of the WIAMan-LX, along with an additional 6-axis load cell below the knee joint of the test rig, recorded the dynamic time-histories of the model. Six DOF accelerometers located in the foot and tibia of the WIAMan measured linear acceleration and rotational velocity with respect to the X-Y-Z axes. Single axis accelerometers aligned with the vertical (Z) axis were placed on the impactor plate to record the input acceleration. The knee load cell was the only common sensor in WIAMan, Hybrid-III and PMHS tests and therefore was used to assess biofidelity.

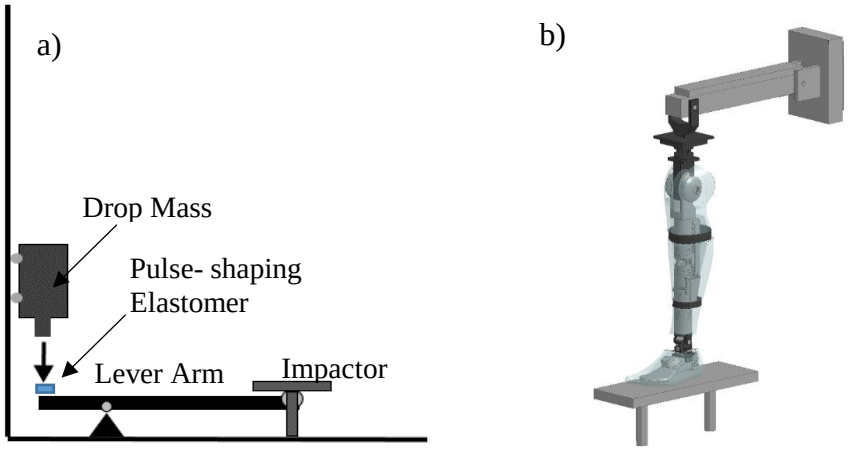

Figure 3.3 (a) Schematic of the drop mass-lever-impactor system and (b) diagram of the Vertical Accelerator (VertAc) device [27] showing the WIAMan-LX attached to the upper femur bar-slider mechanism

The full VALTS system (Fig. 3.4a) is built to simulate under-vehicle events on whole-body specimens[26]. A modified version of this test device was used for standalone lower limb tests (Fig. 3.4b) in which only the foot platen (36 x 59 cm) was loaded. The inferior side of the ATD foot was positioned on top of a foot platen. A pneumatic actuator propels guided ballistic masses into the foot platen to initiate the impact event. Elastomeric dampeners were used to control the magnitude and shape of the input to the foot platen. The target inputs were maximum foot platen velocities of 2, 4, and 6 m/s with peak velocity occurring at 5 ms. Input conditions were tuned based on a linear regression fit of the input parameters recorded during testing. Two tests were performed at each speed to evaluate repeatability. The VALTS rig included two three-axis load cells that were fixed to the foot platen and situated beneath the heel and toe, respectively. One six-axis load cell was fixed above the ATD and below the knee joint. Single axis accelerometers attached to the foot platen captured the vertical acceleration of the impactor.

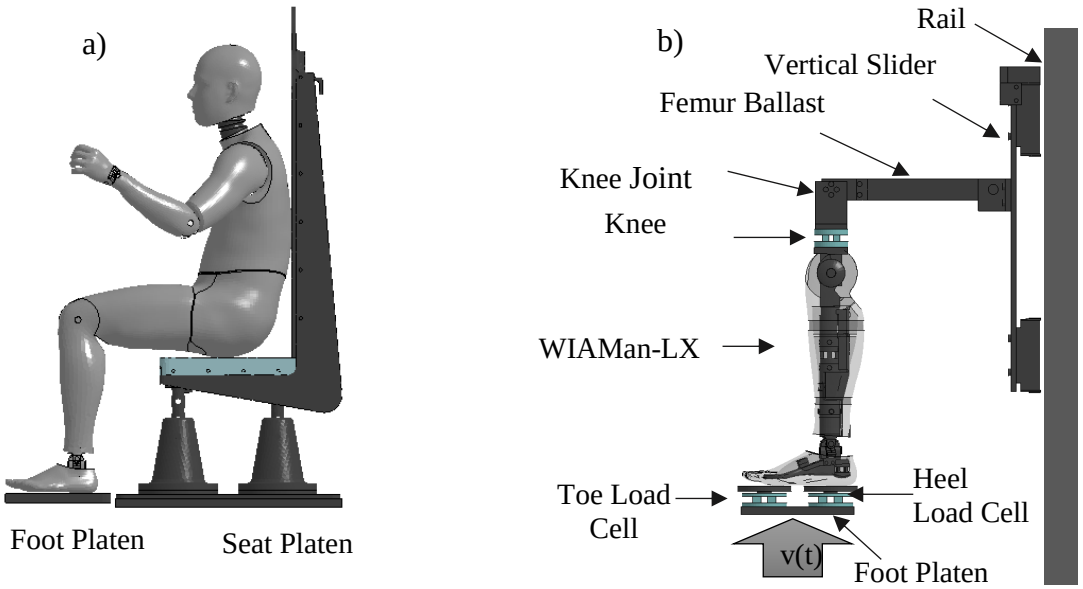

Figure 3.4 (a) Partial VALTS rig for whole body tests showing the separation of the seat and foot platen and (b) diagram of modified VALTS rig for standalone lower limb tests

The validation of leg FE model was performed against the time histories of forces and accelerations along the longitudinal (Z) axis as well as bending moments about the Y axis recorded in testing. Calibrating the model to these signals is done to develop injury risk curves associated with under-body explosions[28]. To comply with the established J211 CFC corridors[29], forces and moments were filtered with an SAE CFC 600 low-pass filter and accelerations were filtered with an SAE CFC 1000 filter. The strength of correlation between the experimental and simulation results were evaluated using the objective rating systems correlation and analysis (CORA)[30] and the recently conceived International Organization for Standardization (ISO) metric[31]. These metrics were developed for comparing ATD responses to finite element predictions with minimal user bias. Responses were compared using both rating systems to analyze the discrepancies between CORA and ISO. The time of evaluation to determine the scores encompasses the entire loading and unloading phase.

The CORA rating system evaluates the correlation of two signals using two independent sub-ratings, a corridor rating and cross correlation rating. The cross correlation rating quantifies similitude of the phase, size, and shape of the signals. The corridor rating calculates differences between the measured response and established corridors. The corridor and cross correlation ratings were designed to compensate for each other's disadvantages. To reduce user bias, CORA scores were calculated based on parameters recommended by the developer.

The ISO rating technique combines the corridor metric from CORA with the Enhanced Error Assessment of Response Time (EEARTH) metric[32]. The total correlation score of the signals is calculated by combining weighted (WCORA = 0.4; WEEARTH = 0.6) sub-ratings from the CORA corridor metric and EEARTH metric. EEARTH measures the error in the phase, magnitude, and topological signal characteristics. Dynamic time warping is used by the EEARTH metric to separate the interaction of phase, magnitude and topological errors. The EEARTH metric is similar to the cross correlation metric used by CORA, except it does not rely on signals defined before and after the interval of evaluation to calculate reliable objective scores.

3.4 Results

The final lower limb model has 212,001 nodes, 164,755 hexahedral elements and 22,027 tetrahedral elements and it was obtained after successive mesh smoothing and mesh convergence studies. Use of tetrahedral elements was confined to the leg flesh, a non-structural component surrounding the tibia shaft. The majority of the FE model elements have high quality (Table 2) within the limits of automotive industry quality mesh criteria[33]. The lower limb model weighs 5.4 kg, matching the weight of the ATD lower limb. The timestep of the model simulations was 0.0446 μs.

Table 3.2 Mesh quality of the WIAMan leg model

Element Type	Mesh Quality Criterion	Min (m)/Max (M) value	Allowable Limit	Elements under/over allowable limit
Shell	Jacobian	0.9 (m)	0.3	0 (0%)
	Warpage	20 (M)	50	0 (0%)
	Aspect Ratio	3.1 (M)	8	0 (0%)
Solid	Jacobian	0.27 (m)	0.3	32 (0.00017%)
	Warpage	63 (M)	50	12 (0.00006%)
	Aspect Ratio	13.4 (M)	8	243 (0.0013%)

Overall, the simplified rubber material models (MAT 181, LS-DYNA) assigned to polymeric components accurately modelled the non-linear strain-rate dependent response of corresponding uniaxial material tests. Engineering stress and strain measurements recorded during simulations were compared to curves obtained from experiments (Fig. 3.5). In experiments, the flesh materials showed negligible strain rate dependency in tension (Fig. 3.5a,e). When developing the model for these two materials, a single curve was used to represent tensile behaviour across the entire range of strain rates.

The WIAMan-LX FE model showed good correlation to the averaged data of 3 tests recorded on the VertAc at an impact velocity of 2 m/s (Fig. 3.6). Correlation scores calculated using both the CORA and ISO methods are provided for each response. The scores are a weighted value between 0 (the worst) and 1(the best) to assess the correlation between the numerical results and corresponding dummy test data. WIAMan and H-III dummy responses were compared to PMHS VertAc experiments to examine their biofidelity. Comparing the axial force at the knee shows the WIAMan is able to closely mimic the human response and replicate the load transfer through the lower limb. The peak force recorded by the WIAMan was 12% lower than the human surrogate. The WIAMan FE model also predicted peak knee axial force 12% lower than the PMHS

response, however the peak occurs slightly earlier. The peak force of the Hybrid-III was 58% higher.

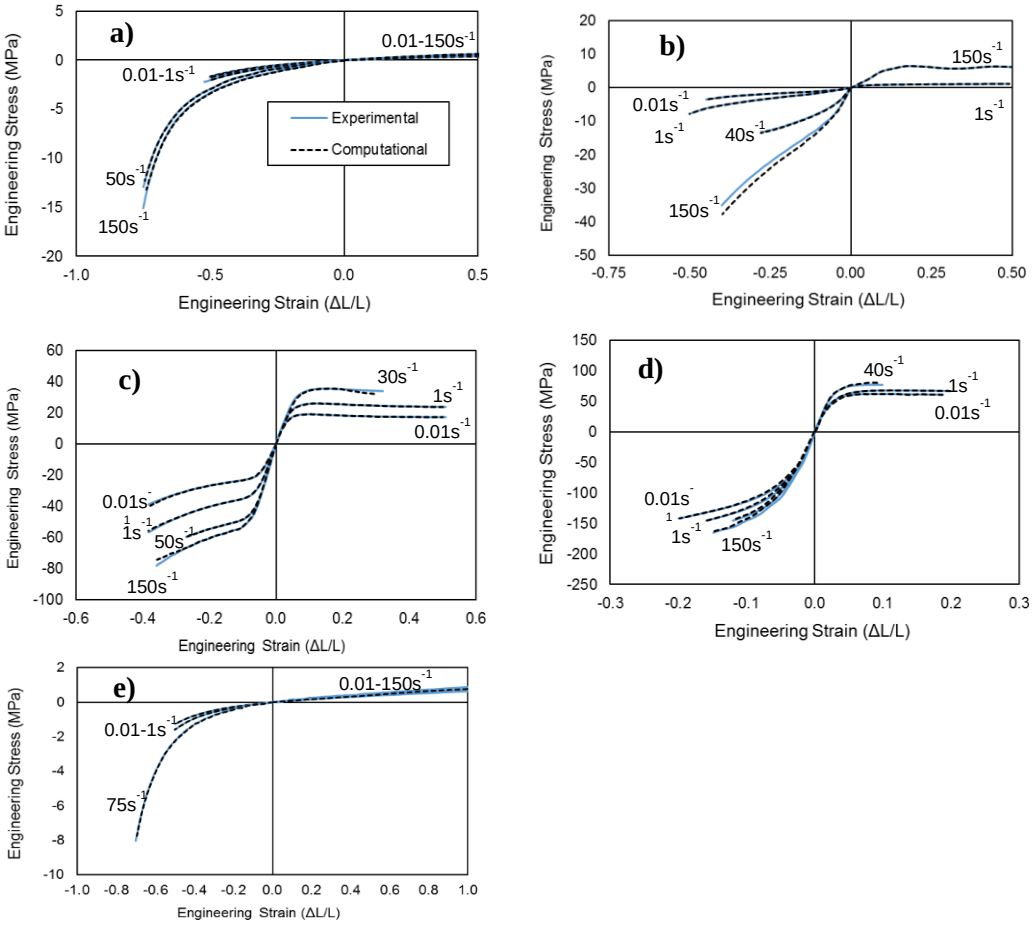

Figure 3.5 Comparison of experimental data and simulation results for viscoelastic materials (a) Foot flesh (b) compliant element (c) footplate (d) calcaneus cap (e) leg flesh

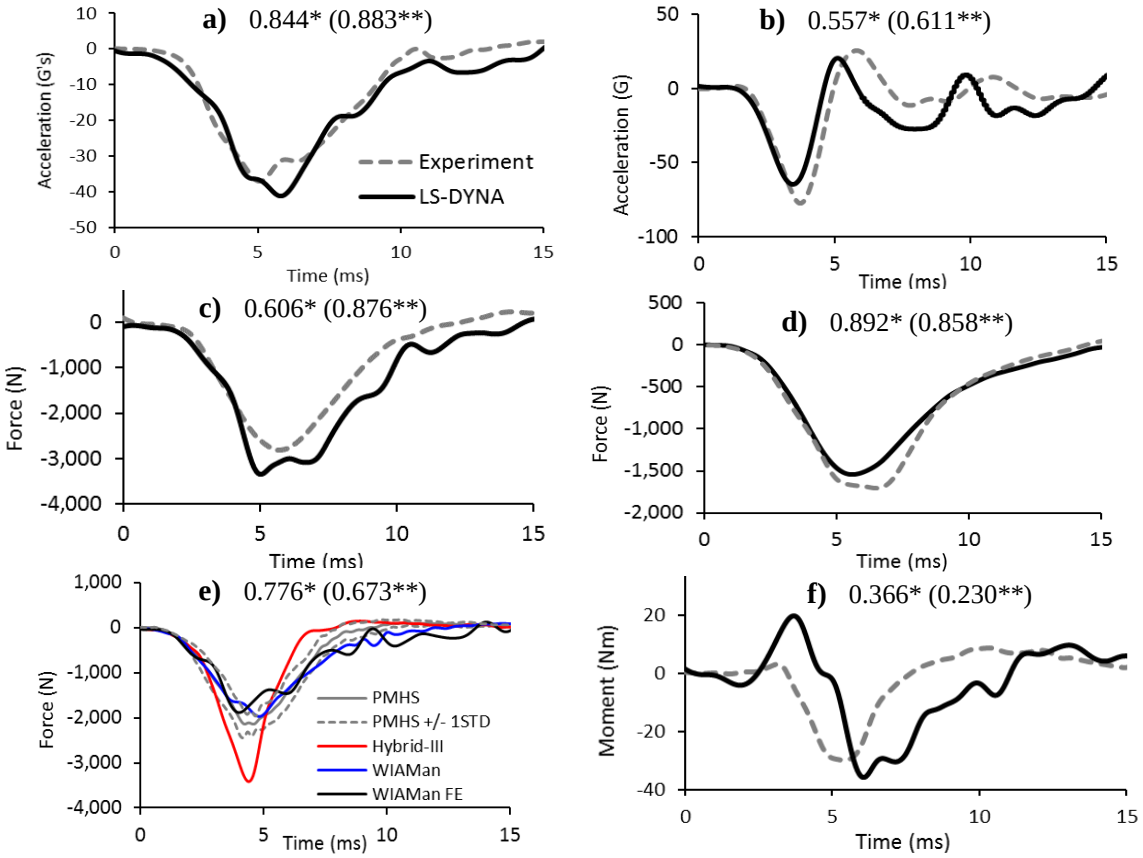

Figure 3.6 Comparison between WIAMAN-LX results and VertAc test data: a) tibia acceleration (z-axis), b) foot acceleration (z-axis), c) knee force (z-axis), d) calcaneus force (z-axis), e) tibia force (z-axis), f) tibia moment (y-axis). Both *ISO score and **CORA scores are provided. Axial (Z) force measured at the knee for Hybrid-III and PMHS tests is also shown to highlight biofidelity improvements of the WIAMan.

A comparison between LS-DYNA simulations and VALTS experiments (Fig. 3.7) shows the WIAMan-LX model is able to accurately replicate the force and acceleration responses of the dummy for pre-impact speeds of 2.4 m/s, 3.9 m/s, and 5.8 m/s respectively.

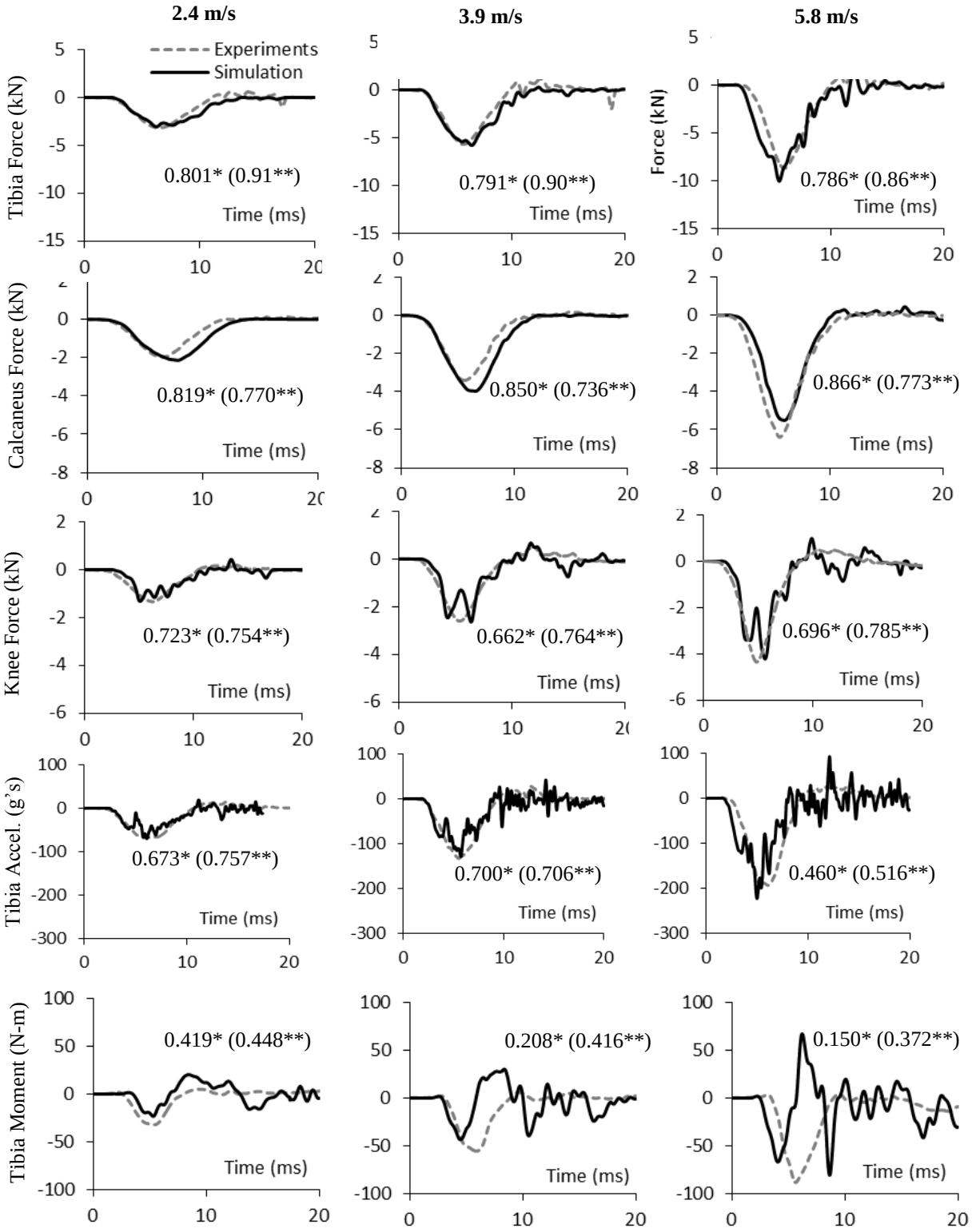

Figure 3.7 Comparing simulations to VALTS experiments at impact conditions of 2.4 m/s, 3.9 m/s, and 5.8 m/s. For each signal are provided both *ISO score and **CORA score

3.5 Discussion

This study presented the development and validation of the WIAMan dummy lower limb FE model. The WIAMan dummy represented a mid-size male solider in a seated posture associated with military vehicle occupants. The lower limb model was built based on CAD geometry of the physical dummy. The entire model was composed of deformable elements to quantify the stress and strain distributions during under-body explosion events. While the material properties of metallic parts were assigned based on literature data, specific tension/compression tests were performed for dummy elastomer parts. Distinct stress-strain curves at various strain rates were observed under compression, the primary loading during under-body explosion events. The foot flesh and leg flesh materials showed negligible rate effects in tension compared to compressive responses. Therefore, a single tension curve was used to represent the tensile stress-strain behaviour for both materials. A simplified rubber material (MAT 181) was chosen due to its ability to simulate non-linear viscoelastic properties of polymers[34]. Other rubber/foam LS-Dyna material models were investigated using optimization-based material identification. However, MAT 181 was the only material model that matched the experimental stress-strain curves for the whole range of tested strain rates. In addition, the elastomer used in the 40 mm compliant element showed the highest strain-rate dependency and highest influence on leg axial stiffness. Therefore, the design of compliant element could be used in the future to better calibrate the physical dummy leg against PMHS tests data performed at a larger range of loading rates (e.g. by optimizing its dimensions).

The model replicated kinematic and kinetic responses of the physical ATD recorded on two test devices (VertAc and VALTS) at four impact velocities (1.9, 2.4, 3.9 and 5.8 m/s). Reasonable predictions of force and acceleration response in the calcaneus, tibia and knee were observed and confirmed by objective rating scores. These locations are commonly used for injury

prediction and will be used in the future to aid in the development of dummy injury risk curves for UBB. A comparison between the CORA and ISO objective rating metrics was shown for each signal used in the validation. Generally, the noisier signals such as the knee force, tibia acceleration and tibia moment received lower ISO ratings compared to CORA ratings of the same signal. This is likely attributed to the sections of the simulation curves where the sign of the slope is opposite that of experimental curve. In contrast, higher ISO scores relative to CORA were given to the axial calcaneus forces. These responses were similar in shape and magnitude, but varied slightly in phase. Visual analysis coupled with the ISO and CORA ratings highlight the improvements of the ISO method.

A comparison of the WIAMan, Hybrid-III and PMHS experiments was shown to assess the biofidelity of the WIAMan and Hybrid-III dummies when struck on the plantar surface of the foot. However, the type and location of the instrumentation used to measure kinematic and dynamic responses the Hybrid-III, WIAMan and human leg surrogates varied due to inherent differences and design challenges. These differences limited the assessment of biofidelity to the load cell integrated to the test fixture, referred to as the knee. Examining the vertical force in the knee, the WIAMan lower extremity showed to be more biofidelic compared to the Hybrid-III, so replacing H-III lower leg dummy with WIAMan in live-fire IED tests is recommended.

It should be mentioned that the WIAMan FE model was validated preliminarily without the inclusion of personal protective equipment (PPE) (i.e. military combat boot) because the objective was to validate a model of the ATD, not a model of the combat boot. Kalra et al. studied the effect of boot compliance using the Hybrid-III. They recommended validating barefoot conditions first due to the major influence of the boot material on the response[35]. A booted validation requires a well-validated FE model of the boot which was not included in the scope of

this work. In addition, a booted leg model increases the complexity of the validation process by accurately re-creating biofidelic contact between the boot and the dummy foot. Therefore, the validation of the WIAMan-LX model with a combat boot is recommended to be performed in future.

The experiments on the physical dummy used in the model validation assumed a neutral (90 degree) angle at the foot and knee. To investigate the sensitivity of the model to the pre-impact leg and foot postures, model sensitivity studies using design of experiments (DOE) with an unbooted and booted lower limb should be performed in the future as well. Furthermore, it is expected that in theatre, vehicle occupants will be situated in different postures from one another. If the load cell in the calcaneus is to be used for assessing risk of heel fracture, the sensitivity of that load cell must also be analysed using the model. Finally, once the validation of the whole ATD model with a combat boot is completed, the FE model could be used to develop a dummy-human transfer function for different loading configurations based on PMHS test data and/or the simulation data using a biofidelic human FE model.

3.6 Conclusion

In this study, the development of a foot and leg finite element model of the WIAMan dummy corresponding to a mid-size male was presented. All dummy parts and joints were modelled with constant stress elements and as surface contacts, respectively. The material models of metallic and elastomer parts were assigned based on literature data, and specific compression/tension tests, respectively. The FE model accurately replicated the physical dummy under axial loading at four impact velocities from 1.9 m/s to 5.8 m/s. Good results of the model backed by high objective rating scores lead to the recommendation to use it in numerical studies

related to dummy design improvements, dummy sensitivity to various impact conditions and/or in the development of injury risk curves corresponding to WIAMan dummy.

3.7 Acknowledgements

The authors are grateful for the financial support from ARL (Army Research Laboratory). Thank you to Corvid Technologies and The Johns Hopkins Applied Physics Lab for the preliminary modelling work that made this project possible. Thank you to WIAMan ATD Development, BIO, as well as Test and Evaluation product team contributions for providing the test data used in the study.

3.8 References

1. Owens BD, Kragh JF, Wenke JC, Macaitis J, Wade CE, Holcomb JB. Combat wounds in operation Iraqi Freedom and operation Enduring Freedom. *J Trauma.* 2008;64:295-299.
2. Bird SM, Fairweather CB. Military fatality rates (by cause) in Afghanistan and Iraq: a measure of hostilities. *International journal of epidemiology.* 2007;36:841-846.
3. Ramasamy A, Harrisson SE, Clasper JC, Stewart MPM. Injuries from roadside improvised explosive devices. *The Journal of trauma.* 2008;65:910-914.
4. Ramasamy MA, Hill CAM, Masouros S, et al. Outcomes of IED foot and ankle blast injuries. *J Bone Joint Surg Am.* 2013;95(5):e25.
5. Pintar FA. Biomedical Analyses, Tolerance, and Mitigation of Acute and Chronic Trauma. 2012.
6. Ramasamy A, Masouros SD, Newell N, et al. In-vehicle extremity injuries from improvised explosive devices: current and future foci. *Philosophical Transactions of the Royal Society B: Biological Sciences.* 2011;366(1562):160-170.
7. *Test methodology for protection of vehicle occupants against anti-vehicular landmine and/or IED effects: RTO-TR-HFM-148.* NATO Research and Technology Organization;2012.
8. *Procedures for Evaluating the Protection Level of Armoured Vehicles - IED Threat.* NATO;2014.
9. Foster JK, Kortge JO, Wolanin MJ. *Hybrid III-a biomechanically-based crash test dummy.* SAE Technical Paper;1977. 0148-7191.
10. Bir C, Barbir A, Dosquet F, Wilhelm M, van der Horst M, Wolfe G. Validation of lower limb surrogates as injury assessment tools in floor impacts due to anti-vehicular land mines. *Military medicine.* 2008;173(12):1180-1184.
11. Newell N, Masouros SD, Ramasamy A, et al. Use of cadavers and anthropometric test devices (ATDs) for assessing lower limb injury outcome from under-vehicle explosions. 2012.

12. Quenneville CE, Dunning CE. Evaluation of the biofidelity of the HIII and MIL-Lx lower leg surrogates under axial impact loading. *Traffic Inj Prev.* 2012;13:81-85.
13. Untaroiu CD, Yue N, Shin J. A Finite Element Model of the Lower Limb for Simulating Automotive Impacts. *Annals of Biomedical Engineering.* 2013;41:513-526.
14. Yoganandan N, Pintar FA, Kumaresan S, Boynton MD. Axial impact biomechanics of the human foot-ankle complex. *Journal of biomechanical engineering.* 1997;119:433-437.
15. Wang J, Bird R, Swinton B, Krstic A. Protection of lower limbs against floor impact in army vehicles experiencing landmine explosion. *J Battlefield Technol.* 2001;4(3):11-15.
16. Funk JR, Crandall JR, Tourret LJ, et al. The Axial Injury Tolerance of the Human Foot/Ankle Complex and the Effect of Achilles Tension. *Journal of Biomechanical Engineering.* 2002;124(6):750-757.
17. Crandall JR, Kuppa SM, Klopp G, Hall G, Pilkey WD, Hurwitz SR. Injury mechanisms and criteria for the human foot and ankle under axial impacts to the foot. *International Journal of Crashworthiness.* 1998;3(2):147-162.
18. Scherer R, Felczak C, Halstad S. Vehicle and Crash Dummy Response to an Underbelly Blast Event. *RDECOM-TARDEC Unclassified Public Release.* 2011.
19. Mckay BJ. Development Of Lower Extremity Injury Criteria And Biomechanical Surrogate To Evaluate Military Vehicle Occupant Injury During An Explosive Blast Event. *Lower Extremity.* 2010.
20. Pandelani T, Sono TJ, Reinecke JD, Nurick GN. Impact loading response of the MiL-Lx leg fitted with combat boots. *Int J Impact Eng.* 2016;92:26-31.
21. Pietsch HA, Bosch KE, Weyland DR, et al. Evaluation of WIAMan Technology Demonstrator Biofidelity relative to Sub- Injurious PMHS Response in Simulated Under-body Blast Events. *Stapp car crash journal.* 2016;60.
22. Reed MP, Ebert SM, Corner BD. Statistical Analysis to Develop a Three-Dimensional Surface Model of a Midsize-Male Foot. *US Army TARDEC.* 2013.
23. Pintar F, Schlick M, Yoganandan N, Voo L, Merkle A, Kleinberger M. Biomechanical Response of Military Booted and Unbooted Foot-Ankle-Tibia from Vertical Loading. *Stapp car crash journal.* 2016;60:247.
24. Kolling S, Bois PD, Benson D, Feng W. A tabulated formulation of hyperelasticity with rate effects and damage. *Computational Mechanics.* 2007;40(5):885.
25. Yoganandan N, Pintar FA, Schlick M, et al. Vertical accelerator device to apply loads simulating blast environments in the military to human surrogates. *Journal of biomechanics.* 2015;48(12):3534-3538.
26. Dooley CJ. *Spinal Response and Injury Association from Whole Body PMHS in the Under Body Blast Loading Environment*, Johns Hopkins University; 2016.
27. Ott K, Dooley C, Wickwire A, Iwaskiw R, Armiger A, Merkle A. Initial Characterization of the Human Response to Vertical Accelerative Loading. Seventh World Congress of Biomechanics; 2014; Boston, MA, USA.
28. Quenneville CE, McLachlin SD, Greeley GS, Dunning CE. Injury tolerance criteria for short-duration axial impulse loading of the isolated tibia. *The Journal of trauma.* 2011;70:E13-E18.
29. Society of Autmotive Engineers, Instrumentation for Impact Test-Part 1-Electronic Instrumentation, (2007).
30. CORA Release 3.6 User 's Manual, (2012).

31. Barbat S, Fu Y, Zhan Z, Gehre C. Objective rating metric for dynamic systems. *Enhanced Safety of Vehicles.* 2013:1-10.
32. Sarin H, Kokkolaras M, Hulbert G, Papalambros P, Barbat S, Yang R-J. Comparing time histories for validation of simulation models: error measures and metrics. *Journal of dynamic systems, measurement, and control.* 2010;132(6):061401.
33. Meng YZ, Pak W, Guleyupoglu B, Koya B, Gayzik FS, Untaroiu CD. A finite element model of a six-year-old child for simulating pedestrian accidents. *Accident Anal Prev.* 2017;98:206-213.
34. Bois PAD, Kolling S, Koesters M, Frank T. Material behaviour of polymers under impact loading. *Int J Impact Eng.* 2006;32(5):725-740.
35. Kalra A, Somasundram K, Shen M, Gupta V, Chou CC, Zhu F. *Effect of Boot Compliance in Numerical Model of Hybrid III in Vertical Loading.* SAE Technical Paper;2016. 0148-7191.

CHAPTER 4 : VALIDATION OF A BOOTED FINITE ELEMENT MODEL OF THE WIAMAN ATD LOWER LIMB IN COMPONENT AND WHOLE-BODY VERTICAL LOADING IMPACTS WITH AN ASSESSMENT OF THE BOOT INFLUENCE MODEL ON RESPONSE

Wade A. Baker[1], Costin Untaroiu[1], Mostafiz Chowdhury[2]

[1]Department of Biomedical Engineering and Mechanics, Virginia Tech, [2]United States Army Research Laboratory

4.1 Abstract

Recent military conflicts have been characterized by an increase in under-body blast (UBB) casualties surviving with severe and debilitating lower limb injuries. Rapid deformation of the vehicle floor during a blast imparts highly dynamic vertical loads to the occupant's lower limb. A novel anthropomorphic test device (ATD) representative of the 50th percentile male soldier is being developed to predict injuries to a vehicle occupant during a UBB. Finite element (FE) models of ATDs have proven to be efficient and accurate in their ability to predict kinematics and loads experienced by the physical device. The main objective of this study was to validate an FE model of the ATD lower limb outfitted with a military combat boot. The boot model was fit to a previously developed model of the barefoot ATD and assigned contacts and material properties based on previous experiments. To validate the model, six tests on the isolated ATD lower limb with boot were simulated. The load transfer capabilities of the FE model were assessed by comparing predicted force-time responses to values obtained experimentally at three load cells aligned along the load pathway. The booted lower limb sub-assembly was then incorporated into a whole-body model of the ATD. Two whole-body experiments were simulated to evaluate lower limb performance in the whole-body. The model performance leads to the recommendation to use it appropriately as an alternative to costly ATD experiments.

4.2 Introduction

Epidemiologic studies of combat wounds in Operation Iraqi Freedom showed that improvised explosive devices (IEDs) were the predominant cause of lower limb injury among US and coalition forces [1,2]. When detonated beneath a vehicle, IEDs often impart blunt vertical loads to the occupant's lower limb by deformation of the vehicle floor[3]. Increased blast survivability has contributed to a rise in amputations and casualties continuing to live with debilitating lower limb injuries[4]. The use of explosive devices to target military vehicles is expected to remain a predominant threat in future conflicts[3]. Therefore, it is necessary to continue pursuing safety countermeasures that can adequately protect vehicle occupants from severe lower limb injuries.

Anthropomorphic test devices (ATDs), commonly referred to as crash dummies, are designed to predict the risk of injury to a human during an impact. Current military vehicle test standards recommend IED survivability be assessed using the Hybrid III dummy[5]. However, the Hybrid III was designed for automotive occupant postures, impact magnitudes, and durations[6], in particular for frontal crash scenarios. Under low to medium severity vertical loading, the Hybrid III leg has been shown to exhibit poor biofidelity compared to post-mortem human surrogate (PMHS) responses and was not recommended for the assessment of blast mitigation countermeasures[7]. The Military Lower Extremity (MIL-Lx) is a standalone lower limb including a foot, ankle and tibia that was designed for use in blast testing. The MIL-LX can replace the standard Hybrid III lower limb in blast tests[5]. While improved biofidelity was demonstrated in vertical loading experiments[8], the MIL-LX was only calibrated with human cadaver data at a single impact speed[9]. Additionally, it was shown that the compliant element in the tibia bottoms out at high severity impact velocities even when outfitted with a military combat boot[10].

Finite element (FE) modeling has proven to be a low-cost and accurate method to predict the responses of ATDs[11,12]. Newell et al developed a low cost axisymmetric model of the MIL-LX capable of predicting peak compressive loads that can be used to assess blast countermeasures[13]. A particular advantage to the development of FE models is the ability to conduct sensitivity and design optimization studies where a large number of experiments would be required[14], or to predict failure modes in the physical dummy structure. A novel ATD, called the Warrior Injury Assessment Manikin (WIAMan) is being developed by the US Army for under-body blast research (UBB) and an FE model of the ATD is concurrently being developed to aid in design and future research[15,16]. The WIAMan is a whole-body ATD with anthropometry representative of a 50th percentile male soldier[17]. The WIAMan lower limb (WIAMan-LL) was designed to be biofidelic in highly dynamic vertical loading scenarios when compared to PMHS responses[18,19].

This study aims to develop and validate an FE model of the booted WIAMan-LL for simulating under-body blast conditions. While the lower limb and combat boot models were previously validated separately[20,21], no study has been performed previously to validate the combined combat boot and WIAMan model. Axial impact experiments performed on the booted WIAMan-LL were simulated to validate the model. The lower limb sub-assembly and combat boot models were then incorporated into a whole-body FE model of the WIAMan[22,23]. Whole-body vertical loading experiments were simulated to further evaluate the performance of the WIAMan-LL model.

4.3 Methods

The FE model of the WIAMan-LL with a military combat boot was validated at multiple stages. A schematic of the methodology for assessment of the booted lower limb as both an isolated sub-assembly and also a component of the whole-body is shown in Figure 4.1.

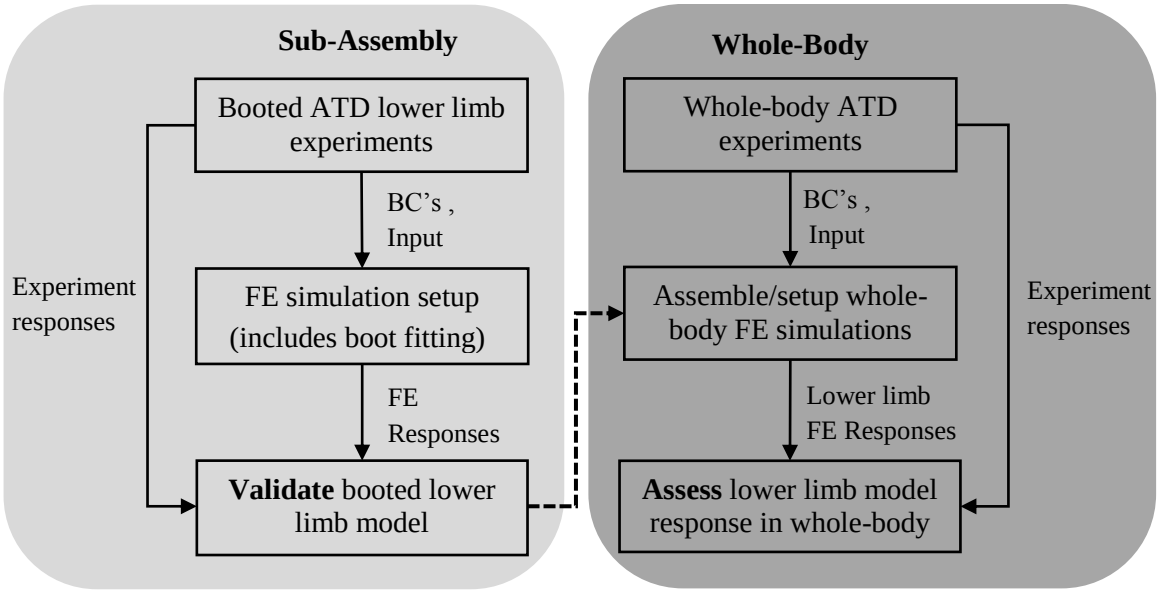

Figure 4.1 The assessment procedure of a lower-limb model with a fitted combat boot as a sub-assembly before incorporating it into a full-body FE model for further assessment.

The FE model of the WIAMan-LL used in this study was developed and validated previously by Baker et al for LS-DYNA (LSTC, Livermore, CA) using barefoot experiments conducting on the isolated lower limb (Figure 4.2a)[20,24]. The mesh was developed from CAD surfaces of the WIAMan ATD[22]. The model contains 100 parts including hardware and instrumentation. Four polymeric components, including a 40 mm compliant element in the tibia shaft, dampen forces entering vertically through the inferior side of the foot (Figure 4.2b). Polymeric components were modeled using a simplified rubber material (MAT 181, LS-DYNA)[25]. The rate-dependent polymer models were developed from uniaxial compression and tension experiments conducted on samples at strain rates of 0.01-1000/s. Material properties for metallic parts were assigned based on values found in literature.

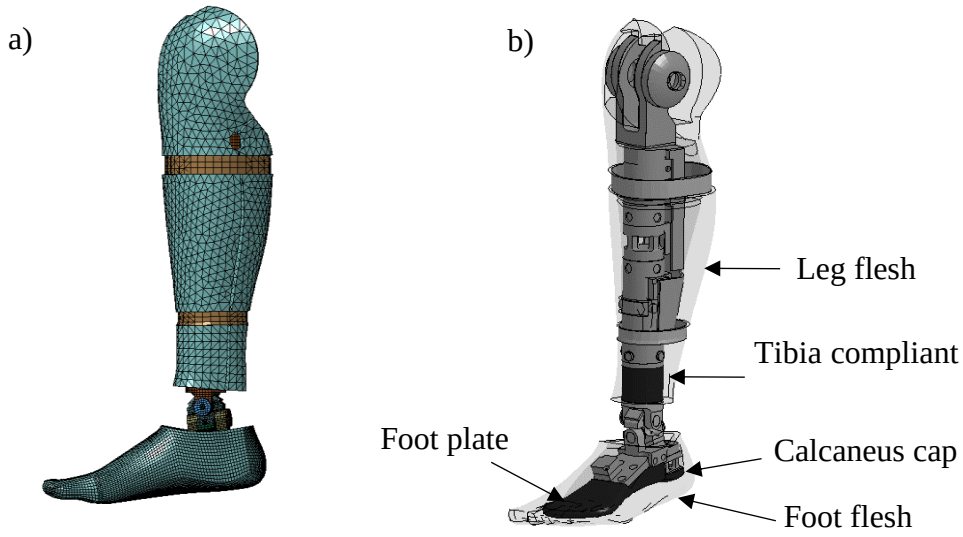

Figure 4.2 (a) Finite element model of the lower limb previously developed and validated [20] (b) Diagram of soft components of the WIAMan lower limb.

A Belleville 390 DES hot weather combat boot (Belleville Boot Company, Belleville, IL, USA) model was built based on a previously developed model of a similar boot (Figure 4.3)[21]. A brief description of the Krayterman model is provided. The boot sole is comprised of the tread, mid-sole and upper sole layers. A fiberglass shank embedded in the midsole and foam insert were modeled as well as the heel cup, toe cup and fabric for the upper part of the boot. The model geometry was developed from 3D surface reconstruction of individual parts. Compressive stiffness of the boot sole was characterized experimentally using drop tower tests on the Compression Test Rig (CTR) similar to floor mat experiments by Sakamoto et al[26]. Material model parameters for the boot mid-sole were obtained through a parameter optimization process in LS-OPT (LSTC, Livermore, CA) by matching simulation predictions to experimental responses of an accelerometer fixed to the CTR. A summary of the LS-DYNA material models and relevant parameters for each component is given (Table 1). The boot tread was glued to the mid-sole in the model using a tied contact. Fabric was connected to the midsole with common nodes.

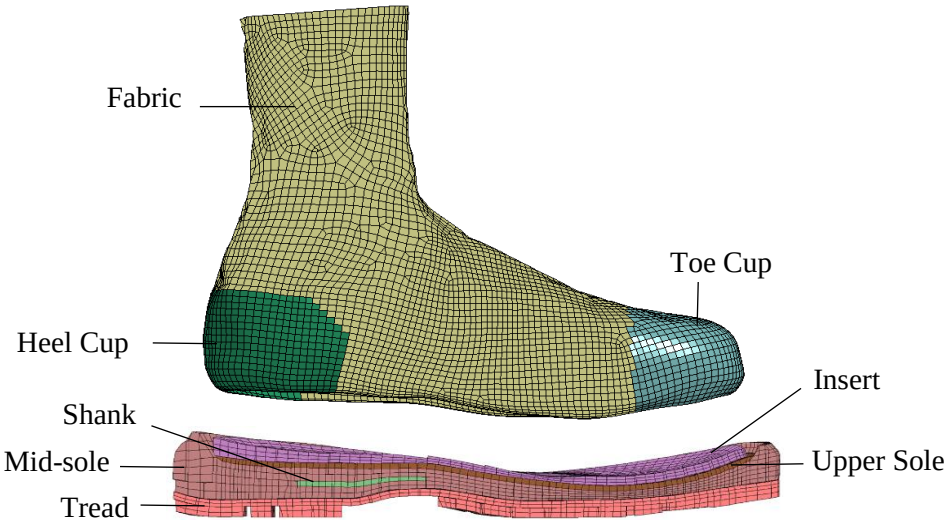

Figure 4.3 Finite Element Model of the Belleville combat boot used in simulations. The upper fabric was separated from the lower boot to show a cross-section of the boot sole.

Table 4.1 Material models and properties and used for the Belleville combat boot

Boot Part	**LS-DYNA Material**	**Density (g/cm^3)**	**Modulus* (MPa)**	**Poisson's Ratio**
Tread	BLATZ-KO_RUBBER	1	15 (G)	N/A
Mid-Sole	VISCOUS_FOAM	0.85	0.5 (E)	0.15
Shank	ELASTIC	2.44	11,000 (E)	0.183
Upper Sole	ELASTIC	0.16	320 (E)	0.25
Insole	LOW_DENSITY_FOAM	0.076	15 (E)	N/A
Heel Cup	ELASTIC	0.96	1500 (E)	0.05
Toe Cup	ELASTIC	0.96	1500 (E)	0.05
Fabric	FABRIC	1.07	13,800 (E) / 10,550 (G)	0.35

* E –Young's modulus, G – Shear modulus

Models of the boot and the WIAMan-LL were imported into the Hypermesh pre-processor (Altair, Troy, MI, USA). The boot model was fit over the foot and leg flesh of the WIAMan-LL using a series of linear and rotational movements. Nodes from the boot fabric were manually adjusted to avoid penetration with the leg flesh. A sliding contact was used to model the interface between the boot insole and the WIAMan with an assumed coefficient of friction of 0.3. The boot fabric was tied to the lower leg flesh to simulate the effect of boot laces.

Experiments conducted with the VALTS test device were simulated to validate the booted WIAMan-LL FE model. The left ATD lower limb was used in experiments and simulations. The VALTS rig was built by Lansmont Corporation (Monteray, CA, USA) to replicate the injurious loading conditions imparted to a vehicle occupant during a UBB[27]. A modified version of the rig was used for standalone ATD lower limb experiments (Figure 4.4). The WIAMan-LL was fixed to the rig using an adaptor (0.8 kg) that prevented rotation of the surrogate about its proximal end. A knee attachment (1.2 kg) located above the adaptor contained a load cell and connected to the femur bar (3kg). The femur bar had pin joints at either end to approximate the knee and hip joints. Linear motion of the proximal end of the femur bar was limited to vertical translation. The WIAMan was outfitted with a Belleville 390 DES combat boot and placed in a "normal" posture meaning 90^{o} angles of the knee and ankle joints. The bottom surface of the boot tread rested on the floor platform. Experiments were simulated where the peak floor plate velocity reached 2, 4, 6, 10 and 12 m/s with a 5-millisecond time to peak (TTP) velocity. An additional condition was simulated for which the peak velocity was 6 m/s and the TTP was extended to 8 milliseconds. Each condition was tested twice and negligible variation was seen between tests.

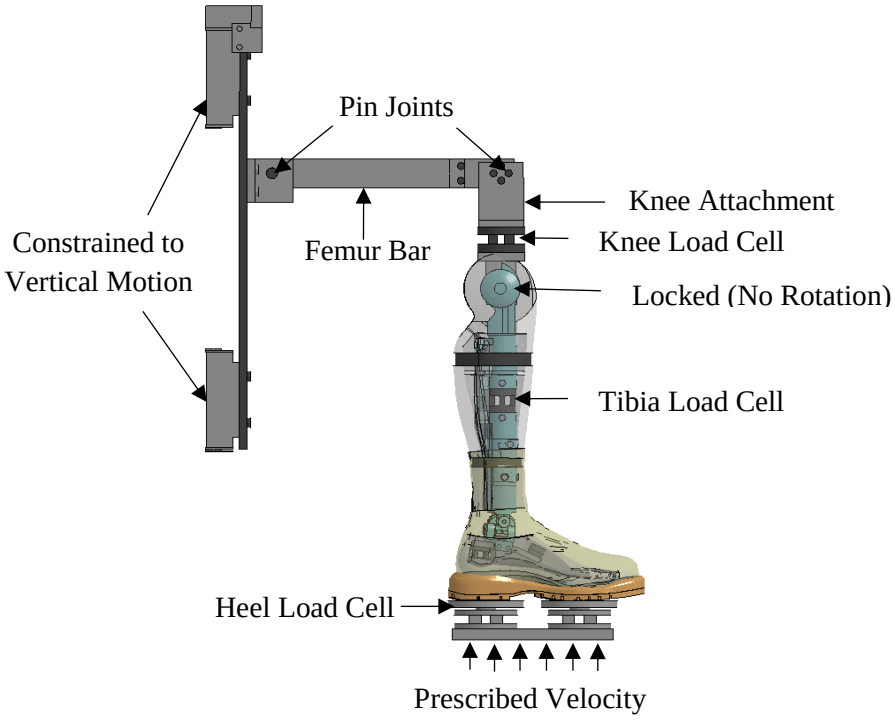

Figure 4.4 Diagram of the setup for VALTS leg experiments and simulations of the isolated WIAMan-LL sub-assembly

Connections between the rig and WIAMan-LL were modeled using contacts that properly represented experimental conditions. Pin joints in the rig were modeled as sliding interfaces. Input to the FE model was the experimental velocity-time history of the floor plate integrated from an accelerometer fixed to the plate. The model was allowed to settle for 150ms prior to prescribing the input velocity to initiate the boot-foot and boot-floor contacts. Experiments were simulated for 30 ms to capture kinematics and loads relevant to validation. Responses from the heel and knee load cells attached to the VALTS device as well as a load cell in the tibia shaft of the WIAMan were used for validation. Predicted axial forces output in the local coordinate system of the instrument were compared to experimental results to assess the capability of the model to accurately transfer loads through the ATD. All forces were filtered at 600Hz in compliance with appropriate standards (SAE J211). Comparison between experimental and simulation results was

assessed using the objective rating metric Correlation and Analysis (CORA) developed for automotive dummy simulations[28]. CORA determines the strength of correlation between simulation and experiment signals by combining a cross-correlation score (based on phase, shape, and magnitude) with a corridor rating score. Values recommended by the developer were used as weighting factors. Only the time interval of the loading and unloading of the ATD was used to compare the signals. Correlation strength was measured on a scale of 0-1 with 1 being a perfect score. The booted results were compared to similar unbooted conditions to assess the effect of the boot on peak forces in the ATD and the correlation between models and experiments.

Following component simulations, the left WIAMan-LL model was incorporated into a whole-body FE model of the WIAMan ATD [23]. Each sub-assembly model (i.e. lower limb, femur, lumbar spine, etc.) was validated prior to assembling the full body model but this study focuses on the lower limb. Experiments conducted using the unmodified VALTS rig[23] were simulated to assess the performance of the lower limb model in the whole-body environment (Figure 4.5). The rig loaded the floor plate and seat independently. Two experimental conditions were simulated. The first condition was a peak floor plate velocity of 4 m/s (5 ms TTP) and peak seat velocity of 4 m/s (5 ms TTP). The second condition was a peak floor velocity of 6 m/s (5 ms TTP) and peak seat velocity of 4 m/s (10 ms TTP). All belt restraints used to secure the ATD in experiments were represented in the model. The model was allowed to settle for 150 ms prior to prescribing the input velocity. After settling, experiments were simulated to 50 ms. Load cells in the calcaneus and tibia as well as an accelerometer in the foot were used to compare computational predictions in the axial direction to experimental responses. Correlation between the experimental and simulation signals was assessed using the CORA metric.

The standalone model of the WIAMan-LL in the modified VALTS rig contained approximately 360,000 elements, had a timestep of 0.045 μs, and took 11 hours to run to completion (without mass scaling). The whole-body model in the VALTS rig contained 3.7m elements and required 70 hours to simulate. The timestep of the whole-body FE model was limited to 0.18 μs by mass scaling. The added mass was 1.7 percent of the total mass and was determined to have negligible influence on the responses. All simulations were run on two Intel Xeon E5-2683 processors (2.1 GHz, 16 cores each).

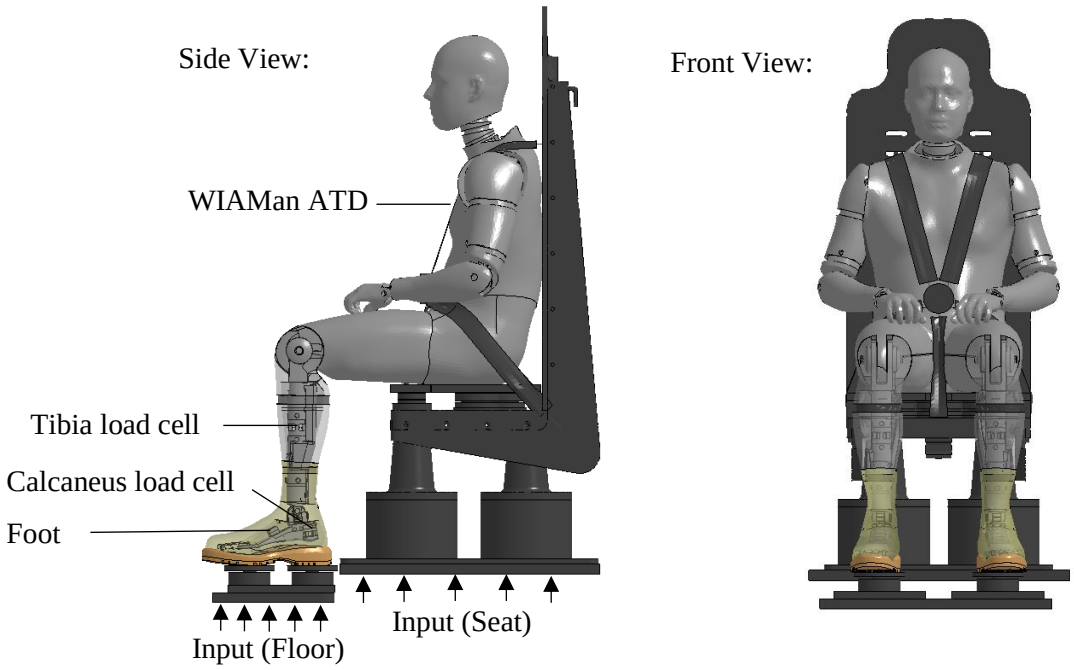

Figure 4.5 Diagram of the WIAMan ATD in a model of the VALTS tests rig used for underbody loading experiments. The dummy lower limb FE model was validated as an isolated component before replacing the lower-limb in the JHU-APL full-body model [23].

4.4 Results

For the isolated component simulations, axial forces calculated at the impactor plate, tibia shaft and upper rig are compared to experimental data (Figure 4.6). Five load severities and two

variations in pulse duration were simulated. Peak experimental and simulation forces along with CORA scores are provided to quantify the strength of correlation (Table 2).

The axial force response in the tibia during unbooted WIAMan-LL experiments and simulations[29] is shown for loading conditions of 2, 4, and 6 m/s (5 ms TTP). Peak forces and CORA scores for unbooted conditions are show along with the booted results (Table 2).

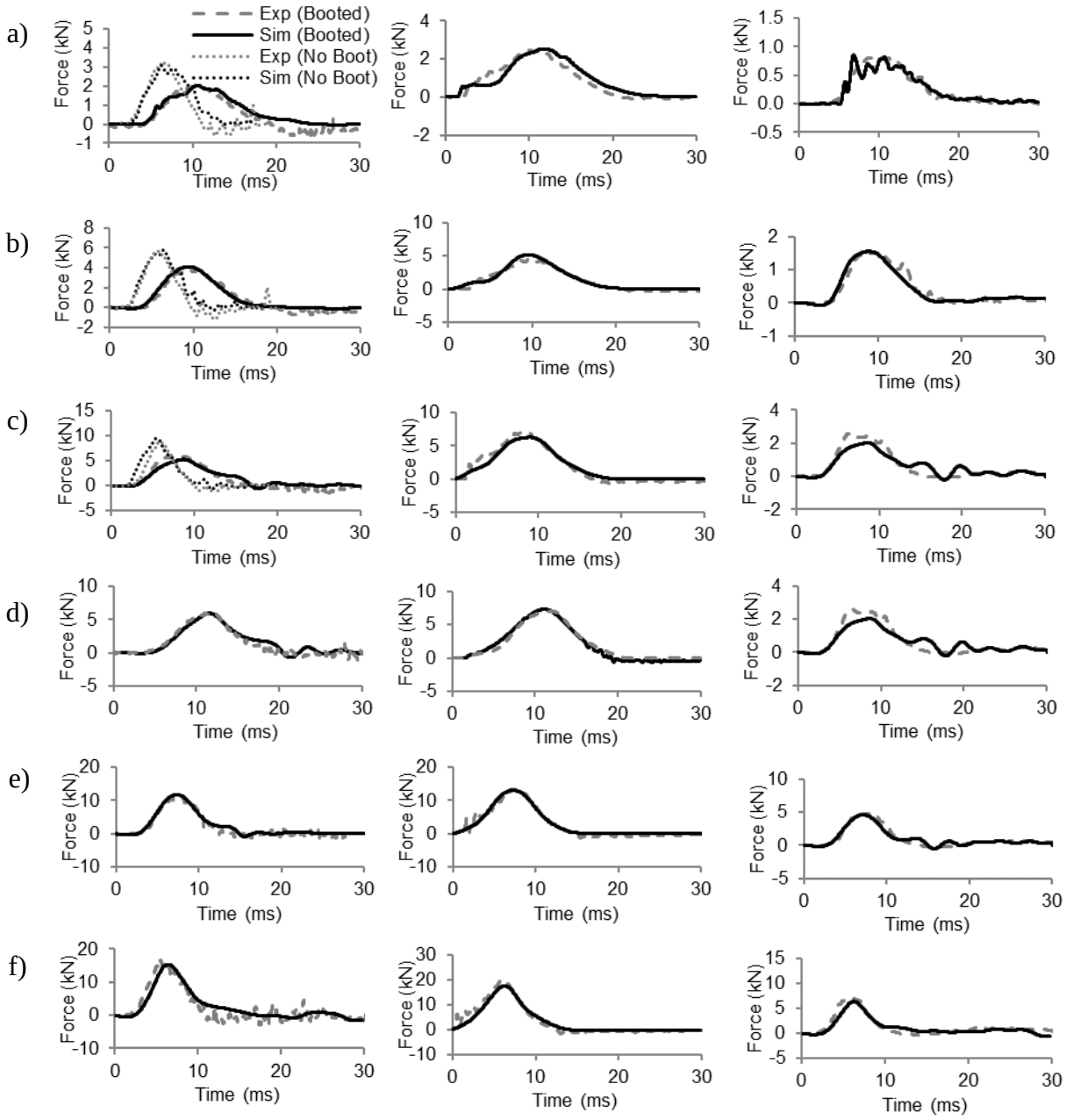

Figure 4.6 Comparing simulations to leg VALTS experiments at impact conditions of (a) 2 m/s, (b) 4 m/s, (c) 6 m/s, (d) 6 m/s (8ms TTP), (e) 10 m/s and (f) 12 m/s. From left to right: tibia, heel and knee axial forces are shown to demonstrate accurate transfer of force through the FE model. Unbooted tibia forces from Baker et al. are shown for 2, 4 , and 6 m/s impacts (5 ms TTP).

Table 4.2 Quantitative comparison of lower-limb model predictions to experimental results in component tests.

Input Conditions	Axial Force Locations	Peak Values Booted (Experiment/ Simulation) (kN)	Booted CORA Score	Peak Values Unbooted (Experiment/ Simulation) (kN)	Unbooted CORA Score
2 m/s - 5 ms TTP	Heel Load Cell	2.45/ 2.54	0.78		
	Tibia Load Cell	1.95/ 2.01	0.93	3.18/ 3.07	0.91
	Knee Load Cell	0.82/ 0.85	0.94		
4 m/s - 5 ms TTP	Heel Load Cell	4.55 / 5.16	0.92		
	Tibia Load Cell	3.88 / 4.11	0.87	5.71 / 5.82	0.90
	Knee Load Cell	1.52 / 1.55	0.87		
6 m/s - 5 ms TTP	Heel Load Cell	7.00/ 6.77	0.87		
	Tibia Load Cell	6.08/ 5.86	0.85	8.72/ 8.63	0.86
	Knee Load Cell	2.61/ 2.13	0.82		
6 m/s - 8 ms TTP	Heel Load Cell	7.34/ 7.08	0.93		
	Tibia Load Cell	6.06/ 5.93	0.92	N/A	N/A
	Knee Load Cell	2.41/ 2.34	0.88		
10 m/s - 5 ms TTP	Heel Load Cell	13.18/ 13.00	0.99		
	Tibia Load Cell	11.72/ 11.80	0.96	N/A	N/A
	Knee Load Cell	4.83/ 4.60	0.90		
12 m/s - 5 ms TTP	Heel Load Cell	17.94/ 17.60	0.85		
	Tibia Load Cell	16.60/ 15.30	0.83	N/A	N/A
	Knee Load Cell	7.23/ 6.40	0.85		

Predictions from the WIAMan-LL in whole-ATD simulations were compared to experimental data (Figure 4.7). Objective rating scores are shown to quantify the model accuracy.

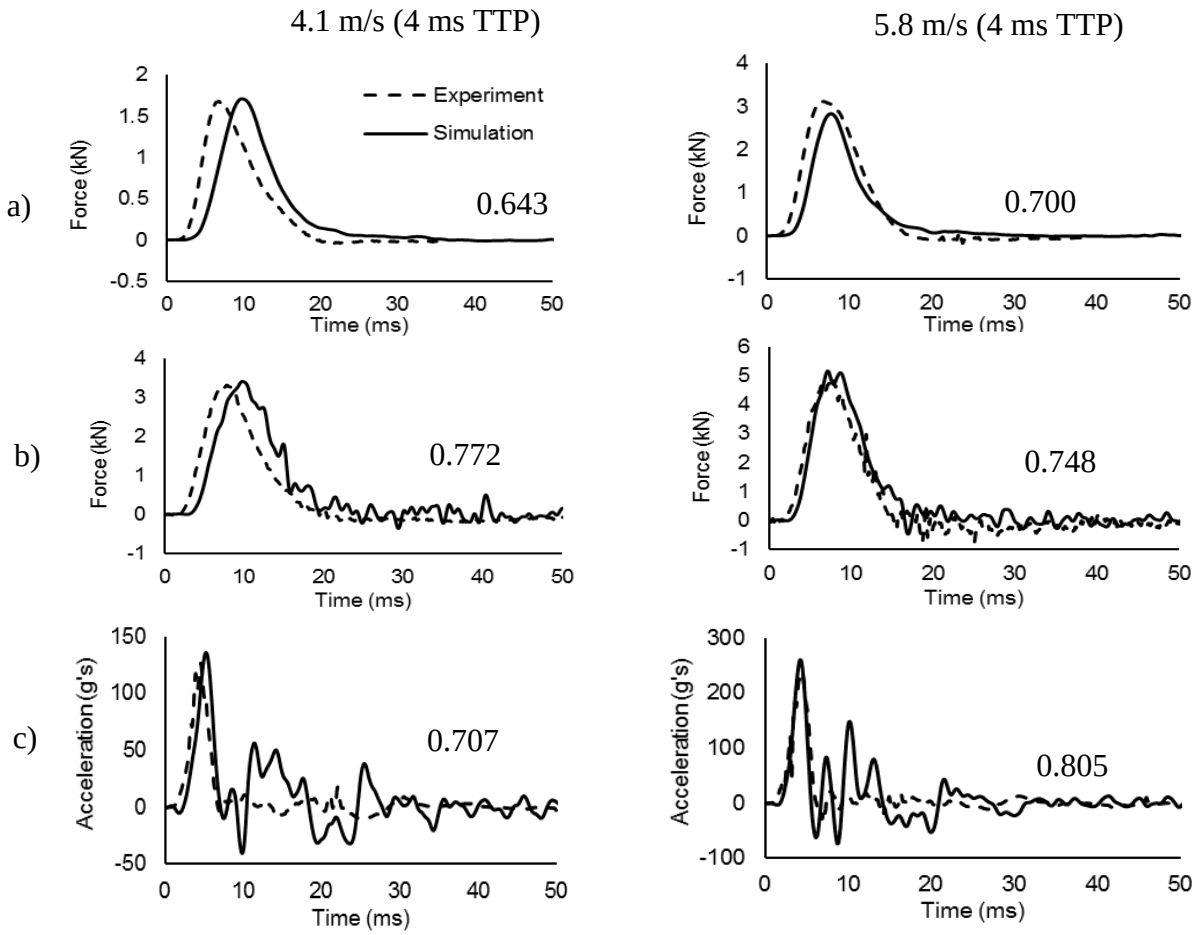

Figure 4.7 Model predictions compared to experimental responses in whole body VALTS experiments. (a) Calcaneus load cell, (b) tibia load cell, and (c) foot accelerometer. Responses from condition 1 are shown on the left and condition 2 on the right. CORA scores are shown for each comparison.

4.5 Discussion

An explicit lower limb model of a novel military ATD has been outfitted with a combat boot and used to simulate under-body blast loading experiments in a military posture. Prior to this study, models of the boot and barefoot ATD were developed and validated separately[21,24]. The booted WIAMan lower limb model was accurate in its ability to predict forces transmitted axially through the device during simulated component tests on the modified VALTS device at five

different impact severities and two input pulse shapes. The average quantitative rating (CORA) for the three load cells across all six conditions was 0.892 (heel), 0.891 (tibia), and 0.877 (knee) with a score of 1 being perfect. All structural parts were modeled using solid deformable elements to predict local stress and strain measurements. While this is useful for design considerations, modeling smaller components such as hardware increases the complexity of model and can induce unwanted noise. However, both the individual and average objective rating scores observed in all experiments are considered high in the context of vehicle safety applications[30]. Results from component simulations show the high accuracy of the lower limb FE model under vertical loading.

The response of the tibia load cell in booted simulations and experiments was compared to unbooted conditions to assess the effects of boot. No experiments on the unbooted lower limb were performed above 6 m/s. Peak forces in booted experiments were reduced 32-39% compared to unbooted experiments. The booted lower-limb FE model accurately reflected the reduction in forces. CORA scores calculated for booted conditions were within +/- 0.03 of the unbooted scores meaning the interaction between the boot and ATD model is considered accurate for this situation.

Furthermore, the performance of the ATD lower limb model, validated with the combat boot, was assessed by simulating two whole-body loading scenarios on the unmodified VALTS rig. Two loads cells aligned with the primary compressive load path were used to show the accurate transfer of loads through the WIAMan-LL. An accelerometer fixed to the ATD foot beneath the flesh validated the kinematic motion of the model. Accurately predicting the axial acceleration of the foot builds confidence in the methods used to model joints in the ankle and knee. The model was able to predict accurately the phase magnitude and shape of the higher severity experimental responses (condition two). For condition one, the phase of the computational response lagged behind the experimental response during loading. This could be attributed to the interaction

between the boot and the foot, which is believed to have a greater effect at lower severity loads. At lower severity floor velocities, it takes longer for the boot and the foot to make a biofidelic connection. The difference in phase was reflected in lower overall CORA scores. While not shown in this study, the responses of the right WIAMan-LL were nearly identical to the left in experiments and simulations. The timestep was limited by mass scaling in order to reduce the simulation time of the model. However, condition one was also simulated without mass scaling and found there was no difference in the lower limb results.

The model of the combat boot used in this study has several limitations that could have affected simulation outcomes. For example, validation of the boot model was mostly focused on tuning the properties of the mid-sole which showed to have the highest influence on the axial boot sole response. The shank, upper sole, heel cup and toe cups were assigned linear material properties based on the assumption that their response plays a negligible role in the overall transfer of energy through the boot and to the leg. A coefficient of friction of 0.3 was approximated for contact between the soft foam insole and the polyurethane foot flesh because no experimental values could be found in literature. A similar study by Nilakantan et al assumed that varying the friction coefficient between the floor and foot would have little effect due to the axial nature of the loading[31]. In the future, improvements to the combat boot model should include updating each component of the sole with strain rate-dependent materials appropriate for blast loading conditions. A more biofidelic interaction between the boot and the leg-foot model should be investigated and employed in future research. It is believed that these future updates will improve the accuracy of the boot model at a higher range of loading conditions.

Vertical loading experiments were conducted on the whole-body WIAMan and human cadavers to preliminarily assess WIAMan biofidelity[19]. These tests showed the right and left

WIAMan lower limbs compared favorably to the human cadavers with CORA scores of 0.622 – 0.818. The validated FE model could provide an inexpensive and reliable tool to assess design changes aimed at improving the ATD biofidelity. The development of a transfer function between the WIAMan and a human will be necessary in the future to assess human injury by interpreting ATD responses. The validated WIAMan-LL model along with validated human limb models could be used in future to develop reliable human-ATD transfer functions to correlate ATD responses with biomechanical injury data related to under-body blasts.

4.6 Conclusion

A novel ATD representative of the average male soldier is being developed to study injury to military vehicle occupants. An FE model of a new ATD lower limb was developed with the inclusion of a military combat boot. The model was first validated as a sub-assembly using tests conducted on the isolated lower limb. Five impact tests were simulated where the booted lower limb was loaded vertically at peak velocities of 2, 4, 6, 10 and 12 m/s. A quantitative comparison of the computational results to experimental responses was done using the CORA rating metric for vehicle safety applications. The model was considered validated when averaged CORA scores were above 0.7. The lower limb model was incorporated into a full body FE model of the ATD. Two experiments on the ATD were simulated to assess the performance of the lower limb in whole body loading environment. The FE model of the lower limb was able to accurately predict axial forces and accelerations measured in all experiments. Therefore, it is recommended that the lower limb model, either as an isolated component or as a part of the full ATD, be used in the future to assess the effectiveness of potential vehicle improvements.

4.7 Acknowledgements

The authors would like to acknowledge the contributions of Corvid Technologies and The Johns Hopkins Applied Physics Lab for providing the baseline ATD models of the lower leg and the whole body that made this project possible. Thank you to WIAMan ATD Development, Bio Mechanics, as well as Test and Evaluation product teams contributions for providing the test data used in the study.

4.8 References

1. Belmont P, Schoenfeld AJ, Goodman G. Epidemiology of combat wounds in Operation Iraqi Freedom and Operation Enduring Freedom: orthopaedic burden of disease. *J Surg Orthop Adv.* 2010;19(1):2-7.
2. Bird SM, Fairweather CB. Military fatality rates (by cause) in Afghanistan and Iraq: a measure of hostilities. *International Journal of Epidemiology.* 2007;36(4):841-846.
3. Ramasamy A, Hill A-M, Hepper A, Bull AM, Clasper J. Blast mines: physics, injury mechanisms and vehicle protection. *Journal of the Royal Army Medical Corps.* 2009;155(4):258-264.
4. Ramasamy MA, Hill CAM, Masouros S, et al. Outcomes of IED foot and ankle blast injuries. *J Bone Joint Surg Am.* 2013;95(5):e25.
5. NATO. Procedures for Evaluating the Protection Level of Armoured Vehicles - Mine Threat. In:2014.
6. Foster JK, Kortge JO, Wolanin MJ. Hybrid III-A Biomechanically-Based Crash Test Dummy. 1977.
7. Bir C, Barbir A, Dosquet F, Wilhelm M, van der Horst M, Wolfe G. Validation of lower limb surrogates as injury assessment tools in floor impacts due to anti-vehicular land mines. *Military medicine.* 2008;173(12):1180-1184.
8. Quenneville CE, Dunning CE. Evaluation of the biofidelity of the HIII and MIL-Lx lower leg surrogates under axial impact loading. *Traffic injury prevention.* 2012;13(1):81-85.
9. Mckay BJ. Development of lower extremity injury criteria and biomechanical surrogate to evaluate military vehicle occupant injury during an explosive blast event. 2010.
10. Pandelani T, Sono T, Reinecke J, Nurick G. Impact loading response of the MiL-Lx leg fitted with combat boots. *International Journal of Impact Engineering.* 2016;92:26-31.
11. Putnam JB, Untaroiu CD, Littell J, Annett M. Finite Element Model of the THOR-NT Dummy under Vertical Impact Loading for Aerospace Injury Prediction: Model Evaluation and Sensitivity Analysis. *Journal of the American Helicopter Society.* 2015;60(2):1-10.
12. Untaroiu C, Shin J, Lu Y-C. Assessment of a dummy model in crash simulations using rating methods. *International Journal of Automotive Technology.* 2013;14(3):395-405.

13. Newell N, Salzar R, Bull AM, Masouros SD. A validated numerical model of a lower limb surrogate to investigate injuries caused by under-vehicle explosions. *Journal of biomechanics.* 2016;49(5):710-717.
14. Putnam JB, Untaroiu CD, Littell J, Annett M. Validation and sensitivity analysis of a finite element model of THOR-NT ATD for injury prediction under vertical impact loading. Paper presented at: AHS International 69th Annual Forum2013.
15. Chowdhury MR, Crawford DM, Shanaman M, et al. *Polymeric Materials Models in the Warrior Injury Assessment Manikin (WIAMan) Anthropomorphic Test Device (ATD) Tech Demonstrator, ARL-TR-7927.* January, 2017.
16. Gibson MW, Armiger RS, Biermann PJ, et al. *Warrior Injury Assessment Manikin (WIAMan) Lumbar Spine Model Validation: Development, Testing, and Analysis of Physical and Computational Models of the WIAMan Lumbar Spine Materials Demonstrator, ARL-TR-7733.* August 2016.
17. Reed MP. *Development of Anthropometric Specifications for the Warrior Injury Assessment Manikin (WIAMan).* DTIC Document;2013.
18. Pintar FA, Schlick MB, Yoganandan N, Voo L, Merkle AC, Kleinberger M. Biomechanical Response of Military Booted and Unbooted Foot-Ankle-Tibia from Vertical Loading. *Stapp car crash journal.* 2016;60:247.
19. Pietsch HA, Bosch KE, Weyland DR, et al. Evaluation of WIAMan technology demonstrator biofidelity relative to sub-injurious PMHS response in simulated under-body blast events. *Stapp car crash journal.* 2016;60:199.
20. Baker W, Untaroiu C, Chowdhury M. Development of a Finite Element Model of the WIAMan Lower Extremity to Investigate Under-body Blast Loads. 14th International LS-DYNA Conference; 2016; Detroit, MI.
21. Krayterman D. *Finite Element Model Development and Validation of the Updated Desert Combat Boot Design.* U.S. Army Research, Development and Engineering Command;2014.
22. Bell C, Lister K, Shirley A, et al. Validation of a Whole Body WIAMan Model for Vehicle Survivability. Paper presented at: The Ground Vehicle Survivability Symposium; Nov. 15-17, 2016; Fort Benning, Georgia.
23. Armiger R, Boyle M, Gayzik F, Merkle A, Chowdhury M. The Development of a Virtual WIAMan for Predicting Occupant Injury and Vehicle Performance. Paper presented at: The Ground Vehicle Survivability Symposium, ; Nov. 15-17, 2016; Fort Benning, GA.
24. Baker W, Untaroiu C, Chowdhury M. Development of a Finite Element Model of the WIAMan Lower Extremity to Investigate Under-body Blast loads. 14th International LS-Dyna Users Conference; 2016; Detroit, MI, USA.
25. Kolling S, Du Bois P, Benson D, Feng W. A tabulated formulation of hyperelasticity with rate effects and damage. *Computational Mechanics.* 2007;40(5).
26. Sakamoto M. *Transfer Relation between the Compression Test Rig and the Anthropomorphic Test Device (ATD) Lower Leg.* DTIC Document;2015.
27. Ott K, Dooly C, Strohsnitter L, et al. Comparison of Human Surrogate Responses in Underbody Blast Loading Conditions. *Stapp car crash journal.* 2015;59.
28. Thunert C. CORA Release 3.6 User's Manual. *GNS mbH, Germany.* 2012.
29. Baker W. *Development and Validation of a Finite Element Dummy Lower Limb Model for Under-body Blast Applications*. Blacksburg, VA, Virgini Tech; 2017.

30. Gehre C, Stahlschmidt S. Assessment of dummy models by using objective rating methods. Paper presented at: 22nd International Technical Conference on the Enhanced Safety of Vehicles, Washington, DC2011.
31. Nilakantan G, Tabiei A. Computational assessment of occupant injury caused by mine blasts underneath infantry vehicles. *International Journal of Vehicle Structures & Systems.* 2009;1(1-3):50-58.

CHAPTER 5 : CONCLUSION

5.1 Contributions

The work in this thesis reflects the effort of the author to model the lower limb of a novel ATD. The ATD was designed for a military anthropometry and posture to be biofidelic under vertical accelerative loads[1]. Other models of the ATD are described in the literature[2,3]. Specific contributions of the author are as follows:

(1) Material characterization tests of eight polymer materials were used to construct rate-dependent finite element materials able to replicate the experimental responses under a large range of applied strain rates (0.01 – 1000/s).
(2) Development of the ATD lower limb model in LS-DYNA including assignment of all contacts, materials and section definitions.
(3) Set-up and simulation of isolated ATD lower limb experiments on two vertical impacting devices. These experiments provided well-defined boundary conditions and initial conditions to facilitate model validation.
(4) Comparison of simulation predictions to experimental results in a total of 10 matched-pair tests to validate the model in conditions similar to the intended operating environment of the ATD.
(5) Assessment of the lower-limb sub-assembly model in simulations of the full ATD.

The novelty of this study includes:

(1) The independent development and validation of a novel ATD lower-limb model. This builds confidence in the verification of similar ATD computation models developed by other project members. In this work, an FE model of the WIAMan-LL was developed starting with the characterization of rate-dependent polymers that make up structural components of the ATD. The response of the ATD to varying severities of blast loads is significantly influenced by the polymer components placed along critical loads paths. The response of the materials in tension and compression was used to develop FE material models that could accurately replicate the rate-dependency observed in

experiments. The polymeric materials were developed in-house and assigned to corresponding components in the ATD FE model.

(2) Validation of the model with and without the inclusion of a military boot. Simulations of vertical impact experiments conducted on two test rigs designed for simulated UBB loading conditions were performed. First, experiments conducted on the barefoot WIAMan-LL were simulated to validate the ATD model. Then the validated model was fit with a combat boot and additional simulations were performed. All models were validated if they could accurately articulate and transfer loads.

(3) Assessment of the lower limb model as part of the full WIAMan FE model. The independently developed lower-limb sub-assembly was added to an FE model of the full dummy. Two experiments on experiments on the full dummy were simulated. The strong correlation between simulation predictions and experimental measurements were backed-up by high objective rating scores.

Overall, the results suggest a model of the ATD lower limb was developed that is capable of replicating the forces and kinematics in the physical dummy in its intended loading environment.

5.2 Future Work

Computational models provide a platform for rapid design studies involving the ATD. In the future, the computational lower limb model, either as an isolated component or as a part of the full ATD, can be used to assess the effectiveness of potential improvements to military vehicles, personal protective equipment, or to the physical ATD. The ATD is a mechanical device that can only approximate the response of a human. A transfer function between the ATD and a human should be developed to correlate ATD responses to human injury. The validated WIAMan-LL model along with validated human limb models could be used in future to develop reliable human-ATD transfer functions to correlate ATD responses with biomechanical injury data related to under-body blasts.

5.2 References

1. Pietsch HA, Bosch KE, Weyland DR, et al. Evaluation of WIAMan technology demonstrator biofidelity relative to sub-injurious PMHS response in simulated under-body blast events. *Stapp car crash journal.* 2016;60:199.
2. Bell C, Lister K, Shirley A, et al. Validation of a Whole Body WIAMan Model for Vehicle Survivability. Paper presented at: The Ground Vehicle Survivability Symposium; Nov. 15-17, 2016; Fort Benning, Georgia.
3. Armiger R, Boyle M, Gayzik F, Merkle A, Chowdhury M. The Development of a Virtual WIAMan for Predicting Occupant Injury and Vehicle Performance. Paper presented at: The Ground Vehicle Survivability Symposium, ; Nov. 15-17, 2016; Fort Benning, GA.